RADIATION EFFECTS OF WEARABLE ANTENNA IN HUMAN BODY TISSUES

Author: Francesc Soler

Director: Dr. Heather Song

University of Colorado Springs, 2014

Abstract

Nowadays humankind live completely surrounded by many wireless devices. Modern society lives and works with wireless applications such as mobile phones, GPS devices or other wireless devices that make our life easier. It means that we are constantly interacting with electromagnetic fields. The study of electromagnetic fields effects on human body is a very important subject, due to the possible health effects that these many electromagnetic fields can cause in humans.

This project is focused on the study of the radiation effects in human tissues from one particular antenna. This antenna is a wrist wearable dual-band antenna. The particularity of this antenna is that is the first wrist wearable antenna which transmits distress signals alerts (Beacons) and at the same times receives GPS signals in a wearable PLB (personal locator beacons) device.

In this project the antenna has been reproduced in HFSS and then several studies about the radiation effects have been done. In order to know if the antenna is totally safe, SAR (Specific Absorption Rate) and temperature increase have been calculated for different human tissues.

This has been done for different parts of body such as arm and head. It has been considered that this kind of antenna is always close to the arm because is a wrist wearable device, but that it would be also important to know what happens if the antenna is close to other part of the body, specially head.

Some interesting results, related with SAR and temperature rise has been found in this project. To obtain trustable results about the temperature increase in the different tissues simulated, the Bio-Heat Equation (by Pennes) has been used. All the simulations run, results and conclusions obtained are presented in this report.

Acknowledgments

This project would not exist without the support and the guidance of my supervisor. I would like to thank Dr. Song for giving me the opportunity to do this project in UCSS. I would also like to thank Mr. Rifahh Alkhamis who provided me a lot of material about his Thesis and his antenna. Finally I would like to thank Tangid Onik, a master student of UCSS, who helped me during one part of my project.

Francesc Soler

Table of contents

Abstract 1

Acknowledgments 2

Table of contents 3

Figures 5

Tables 7

I. INTRODUCTION 8

1.1 Radiation and Frequency Spectrum 8

1.2 Antenna Radiation Effects 9

1.3 Specific Absorption Rate 10

1.3.1 SAR. Definition and equation 10

1.3.2 SAR Limits 11

1.4 HFSS SAR Calculator. Local SAR and Average SAR 11

1.5 Rise of temperature in human tissues 12

1.5.1 Short time exposure 12

1.5.2 Long time exposure 13

1.6 Dual-band wrist wearable pi-shaped antenna 14

1.7 Main Goals 15

II. HFSS. First simulations and SAR calculations 16

2.1 Pi-shaped antenna in HFSS 16

2.2 SAR simulations in HFSS 20

III. Design of human body parts 24

3.1 The arm 24

3.2 The head 27

3.3. Arm and head 31

IV. Results I. SAR HFSS Results 33

4.1 Arm tissues SAR Results 33

4.2 Head tissues SAR results 35

4.3 Head and Arm tissues together SAR results 36

V. Results II. Increase of temperature 40

5.1 Short time of exposure to EM fields 40

5.1.1 Increase of temperature in arm tissues 40
5.1.2 Increase of temperature in head tissues. 41
5.2 Long exposure time to EM fields 42
5.2.1 Rise of temperature in long time exposure to EM fields 42
5.2.2 Increase of temperature of head tissues 44
VI. Results III. Other results 52
6.1 Arm tissues. Power vs. SAR 52
VII. CONCLUSIONS AND FUTURE WORK 59
References 61

Figures

Figure I.1 Frequency Spectrum 9
Figure I.2 Mr. Alkhamis Pi-shaped optimized antenna 14
Figure II.1 Example of dipole λ/4 at designed in HFSS 16
Figure II.2 Design of optimized pi-shaped antenna in HFSS 17
Figure II.3 S_{11} parameter of optimized pi-shaped antenna 17
Figure II.4 Radiation pattern of rE at 406MHz 18
Figure II.5 3D plot of realized gain of the antenna at 406 MHz 18
Figure II.6 Radiation pattern of rE at 1575MHz 19
Figure II.7 3D plot of realized gain of the antenna at 1575MHz 19
Figure II.8 SAR simulation at 406MHz of wrist done by Mr. Alkhamis. 20
Figure II.9 Average SAR of brain layer in plane YZ of the half-wave dipole at 406MHz 21
Figure II.10 Local SAR of brain layer in plane YZ of the half-wave dipole at 406 MHz .. 22
Figure II.11 Comparison between Average SAR and Local SAR in the line crossing the spheres 22
Figure III.1 Picture of arms with different layers by [20] 24
Figure III.3 6-layers arm model in 3D view 25
Figure III.2 6-layers arm model in XY plane (left) and XZ plane (right) 25
Figure III.4 Layers of human head by [24] 27
Figure III.5 Six spheres of the six-layer head model 28
Figure III.6 Final 3D head model designed in HFSS 29
Figure III.7 . 6-layers head model in XY plane (left) and XZ plane (right) 29
Figure III.8 6-layers head model in 3D view 30
Figure III.9 HFSS design of arm, head and antenna in XZ plane (left) and in XY plane (right) 32
Figure III.10 HFSS design of arm, head and antenna in 3D view 32
Figure IV.1 Average SAR in skin tissue at 406MHz 33
Figure IV.2 Average SAR in skin head tissue at 406MHz 35
Figure V.1 Time evolution of the increase of temperature in skin head tissue 48
Figure V.2 Time evolution of the increase of temperature in fat head tissue 48
Figure V.3 Time evolution of the increase of temperature in bone head tissue 48
Figure V.4 Time evolution of the increase of temperature in dura head tissue 49
Figure V.5 Time evolution of the increase of temperature in CSF head tissue 49
Figure V.6 Time evolution of the increase of temperature in brain head tissue 49
Figure VI.1 Average SAR vs Power of the three most affected arm tissues at 406MHz 53
Figure VI.2 Average SAR vs Power of the three other arm tissues at 406MHz 53
Figure VI.3 Local SAR vs Power of the three most affected arm tissues at 406MHz 54
Figure VI.4 Local SAR vs Power of the three other arm tissues at 406MHz 54

Figure VI.5 Average SAR vs Power of the three most affected arm tissues at 1575MHz 56
Figure VI.6 Average SAR vs Power of the three other arm tissues at 1575MHz..... 56
Figure VI.7 . Local SAR vs Power of the three most affected arm tissues at 1575MHz . 57
Figure VI.8 Local SAR vs Power of the three other arm tissues at 1575MHz..... 57

Tables

Table I.1. Optimized pi-shaped antenna sizes 15
Table II.1 S_{11} values and bandwidth in working frequencies 17
Table III.1 Arm tissues mass density and thickness [14] 26
Table III.2 Arm tissues parameters at distress signal frequency (406MHz) 26
Table III.3 Arm tissues parameters at GPS frequency (1575MHz) 26
Table III.4 Head tissues mass density and thickness [14] 30
Table III.5 Head tissues parameters at distress signal frequency (406MHz) 30
Table III.6 Head tissues parameters at GPS frequency (1575MHz) 31
Table IV.1 Average and local SAR results at 406MHz and 5 W 34
Table IV.2 Average and local SAR results at 1575MHz and 1mW 34
Table IV.3 Average and local SAR results at 406MHz and 5 W 35
Table IV.4 Average and local SAR results at 1575MHz and 1mW 36
Table IV.5 Average and Local SAR values in arm and head tissues at 406MHz and 5 W 37
Table IV.6 Average SAR levels in the 12 body tissues for Arm and head together and separately and difference 38
Table IV.7 Local SAR levels in the 12 body tissues for Arm and head together and separately and difference 38
Table V.1 Heat capacity of the 6 arm tissues 41
Table V.2 Increase of temperature of arm tissues at 550ms 41
Table V.3 Heat capacity of the 6 head tissues 42
Table V.4 Increase of temperature of arm tissues at 550ms 42
Table V.5 Head Tissues parameters 45
Table V.6. Blood perfusion parameters 45
Table V.7 Maximum rise of temperature for head tissues at 406 MHz 46
Table V.8 Sphere radius of six-layers head 46
Table V.9 Temperature Rise of the six tissues in 3 different time values. 50
Table V.10 Comparison of rise temperatures at 550ms using linear relation and using the bio-heat equation 51
Table VI.1 Average SAR for 1 to 10 W at 406MHz 52
Table VI.2 Local SAR for 0.1 to 50mW at 406MHz 52
Table VI.3 Average SAR for 0.1 to 50mW at 1575MHz 55
Table VI.4 Local SAR for 0.1 to 50mW at 1575MHz 55

I. INTRODUCTION

This research project is mainly focused on the study of the radiation effects of one particular antenna in human tissues. This antenna was designed by a student of UCCS who also manufactured it. The antenna has pi-shaped form and is a wrist wearable dual-band antenna which works transmitting beacon distress signals at 406 MHz and also receives GPS signal at 1575MHz.

In order to understand better the main goals and some important concepts, in this first chapter, some concepts related with antenna radiation and radiation effects are defined and presented.

1.1 Radiation and Frequency Spectrum

Radiation is the energy propagation as electromagnetic waves or subatomic particles through vacuum, space or some material. The radiation is the propagation of energy through a combination of oscillating electric and magnetic fields; the radiation produced as electromagnetic fields is called electromagnetic radiation [1].

The electromagnetic spectrum is defined as the distribution of the electromagnetic waves, from gamma ray, with a wavelength measured in picometers, to radio waves, with wavelengths that can be of kilometers [2].

There are two different main kinds of radiation. The ionizing radiation is the one that has enough energy to break chemical bonds. This kind of radiation has high energy and is able to strip off electrons and, in case of very high-energy radiation, to break up the nucleus of atoms. Ionization is the process in which a charged part of a molecule is given enough energy to break it away from the atom[3]. Some examples of ionizing radiation are ultraviolet radiation, x-ray and gamma rays.

The non-ionizing radiation refers to the kind of electromagnetic radiation that does not have enough energy to ionize atoms or molecules. This kind of radiation has enough energy to move atoms or make them vibrate, but does not have enough energy to remove electrons [2]. Some examples of non-ionizing radiation are sound waves, visible light and microwaves. The frequency spectrum and the two different kinds of radiation can be observed in Figure 1.1.

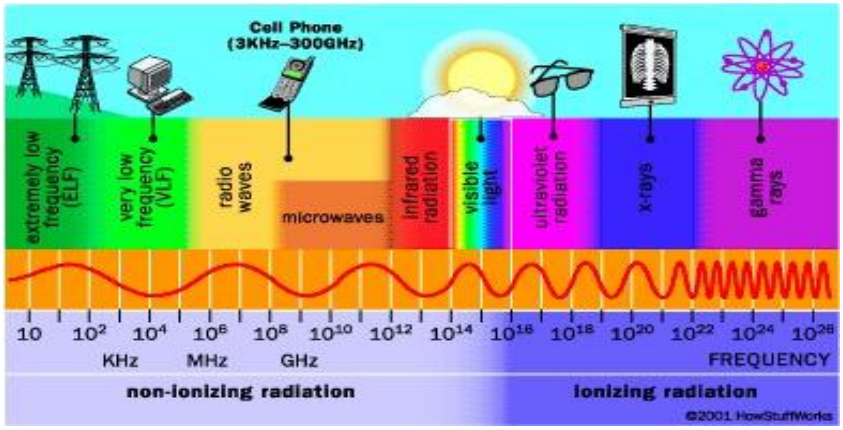

Figure I.1 Frequency Spectrum

1.2 Antenna Radiation Effects

This project is focused on the study of radiation effects of Antenna in Human Tissues. The fact that the working frequencies of the antenna chosen for this project are both in microwave range (406 MHz and 1575 MHz) means that the kind of radiation and radiation effects that will be studied is non-ionizing radiation.

Some of the most important non-ionizing radiation effects in human body are explained in this section. Even though the non-ionizing radiation has not enough energy to modify atoms or human cells, it can have enough energy to move human cells and increase the temperature of these cells. The increase of temperature is a very important factor due to the fact that a high increase of temperature might cause dangerous effects to human tissues.

The most important effect caused by non-ionizing radiation is the dielectric heating. Dielectric heating is a thermal effect caused by microwave radiation that happens when a dielectric material is heated by rotations of polar molecules induced by the electromagnetic field [4].

A part from that, other effects caused by microwave radiation such as cancer, cognitive effects, sleep effects, brain glucose consumption or sperm quality have been studied and report, even some of them have not been scientifically proven.

The increase of temperature of human tissue cells can be explained because a part of the microwaves transmitted by an antenna are absorbed by the body. The tool that measures the rate at which energy is absorbed by human tissues and it is called Specific Absorption Rate (SAR).

1.3 Specific Absorption Rate

1.3.1 SAR. Definition and equation

The metrics of specific absorption rate (SAR) in biological systems or tissue models have been adopted as the dosimetric quantities, especially at RF frequencies [5]. Regarding the antenna works in RF, specific absorption rate is a basic tool or rate in this project.

The Specific Absorption Rate (SAR) is defined as the rate at which RF electromagnetic energy is imparted to unit mass of biological body. SAR is a measure of the rate at which energy is absorbed by the human body when exposed to a radio frequency (RF) electromagnetic field [6]. Thus, SAR measures exposure to fields between 100 kHz and 10 GHz.

To calculate SAR, it is necessary to know the induced field (in V/m) that affects a tissue. Then, SAR is calculated as:

$$SAR = \frac{\sigma \cdot |E|^2}{\rho_m}$$

In the above formula, E is the RMS value of the induced field (in V/m), σ is the tissue conductivity (in S/m) and ρ_m is the mass density of the tissue (kg/m^3).

In case of short exposure times, this does not cause significant convective or conductive heat contribution to tissue temperature rises. Then, in this case SAR can also be expressed as:

$$SAR = \frac{c \cdot \Delta T}{\Delta t}$$

In the formula, c is the heat capacity of the tissue (in J/kg/K) ΔT is the temperature rise (in K) and Δt is the short time exposure (in seconds). As explained in [5], this is true during the initial or transient temperature response curve, in which the relation between temperature rise and SAR is lineal.

1.3.2 SAR Limits

Since some years ago, some authorities have established limits for exposure to radio frequency energy. These limits establish the permitted levels of RF energy for the population. There are two different main authorities who have established two different limits that are not directly comparable.

On one hand, the Federal Communications Commission (FCC) of the U.S. Government established the SAR limit to 1.6 W/kg averaged over 1 gram of actual tissue.

On the other hand, the Council of the European Union established the limit to 2.0 W/kg averaged over 10 g of actual tissue [7].

Due to the fact that these limits are calculated averaging different amount of tissue, the two limits are not directly comparable.

1.4 HFSS SAR Calculator. Local SAR and Average SAR

High Frequency Structural Simulator (HFSS) is a finite element method solver for electromagnetic structures (from Ansys Company). This tool is basically used for antenna design and the design of RF electronic circuits elements [8].

HFSS provides a SAR calculator. It is a very useful tool that allows calculating SAR in tissue volumes. HFSS calculates two types of SAR Field Overlay plots: Local SAR and Average SAR.

Local SAR is calculated using the first equation and at each mesh point on an overlay plot. In the case of Average SAR, it reports the SAR averaged over a volume that surrounds each mesh point [9].

It must be said that HFSS allows defining some SAR settings as the mass of the material that surrounds each mesh point. In order to obtain Average SAR values comparable to the U.S. limit, for all the simulations done in this project, this parameter has been set to 1g.

1.5 Rise of temperature in human tissues

Specific Absorption Rate is a good rate to measure the effects of the EM radiation in human tissues, but sometimes it is not enough. It can be thought that a high level of SAR in any tissue above the SAR limits (1.6 W/kg in U.S.) means directly that the device or antenna is dangerous for human use. To conclude that, it is necessary to know the time of exposure of tissues to EM fields and to obtain the increase of temperature of the tissues.

Thus, it is necessary to obtain the increase of temperature of the tissues to finally conclude if the radiation effects are dangerous for human use or not.

In a paper written in Peru [10] it is explained that the limit of temperature increase in head tissues is 1 K. It is also explained that this increase of temperature in head tissues may affect the behavior and memory of people, before causing anatomical injuries.

In addition, in [11] a deep study about the radiation effects in eye tissue is done. In this paper is mentioned that an increase of temperature at eye tissue higher than 1 K could damage it.

For this reason, in this project it has been considered that an increase of temperature equal or higher than 1 K could be dangerous for any of the human body tissues.

1.5.1 Short time exposure

In case of a short exposure time of high frequency EM radiating to human tissues (not more than few seconds), it is possible to obtain the increase of temperature using the linear relationship seen in Section 1.3.1. To obtain the increase of temperature, it is necessary to know the heat capacity (J/(Kg·K)) of the tissue, the average SAR value in that tissue and the time exposure of EM fields to the tissue. Then, the formula is:

$$\Delta T = SAR \cdot \frac{\Delta t}{c}$$

1.5.2 Long time exposure

In case of long exposure time of high frequency EM to human tissues it is not possible to use the linear relation between ΔT and SAR. To obtain the transient case and the evolution time of the temperature increase for long time of exposure it is necessary to use another equation.

Bio Heat Thermal equation

The thermal model which relates the increase of temperature in function of time and position and considers the thermoregulation and the blood flow of the tissue, is the bio-heat transfer equation found out by Pennes [12] [13]. The bio-heat equation makes possible to find the time distribution, $T(t, r)$.

The bio-heat differential equation modeled by Pennes in 1948 is:

$$\rho c \frac{\partial T}{\partial t} = \nabla(k \nabla T) + \rho Q + \rho S - \rho_b c_b \rho \omega (T - T_b)$$

In the bio-heat Pennes equation, ρ is the mass density of the tissue (kg/m^3), c is the heat capacity of the tissue (J/(Kg·K)), k is the thermal conductivity of the tissue (W/m/˚C). Q is the power generated per unit mass by methabolic processes and S is the SAR due to EM fields radiation (W/kg). T_b is the body core temperature and T is the final temperature considering the EM fields exposure.

Finally, ρ_b and c_b are the blood mass density and the blood heat capacity, and ω is the blood perfusion rate. Blood perfusion rate is the volume of blood flowing through unit mass of tissue per minute (ml/g/min).

It must be said that in thermal modeling of tissue, it is extremely important to describe correctly of the heat transport related to blood flow. Cold blood entering a heated volume of a tissue will cool the tissue [12]. Thus, to solve this equation is really important to know exactly the blood parameters in that body part.

In conclusion, to obtain the evolution time of the temperature increase and to obtain the temperature rise of tissues in function of time or position, it will be necessary to solve, in some way, the bio-heat differential equation.

1.6 Dual-band wrist wearable pi-shaped antenna

This project is focused on the study on the radiation effects in human tissues of one particular antenna. As explained before, the antenna analyzed is an antenna designed by Rifaah Alkhamis, student of UCCS, who designed this antenna in his Master Thesis.

Mr. Alkhamis' antenna is a wrist wearable dual-band antenna. The novelty of this antenna is that is the first wrist wearable antenna which transmits distress signals alerts (Beacons) and at the same times receives GPS signals in a wearable PLB (personal locator beacons) device [14].

This antenna is able to transmit distress signals alerts at 406 MHz with a feeding power of 5 W. At the same time, the antenna can receive GPS signals (at 1575 MHz) of 1mW.

The design of the antenna is pi-shaped form. The pi-shaped form, based in a dipole with two pi-ends lines and a feed line, makes possible that the antenna can transmit beacons and receive GPS signal at the same time.

In this project, the simulated and analyzed antenna is the final optimized pi-shaped antenna that Mr. Alkhamis designed and manufactured in copper and Rogers RT/duroid 6010 substrate. The design of the antenna can be observed in the Figure 1.2. In Table 1.1, all the sizes of the optimized pi-shaped antenna are presented.

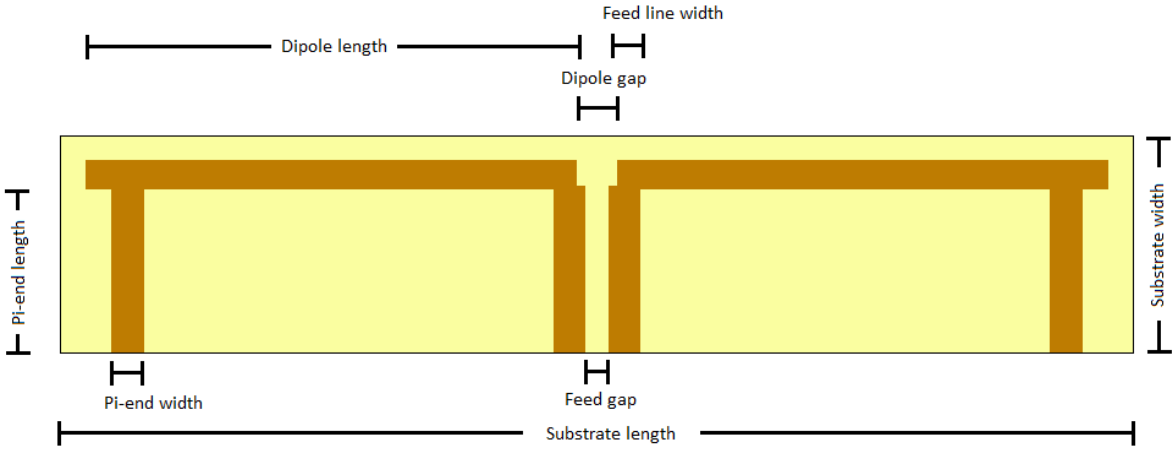

Figure I.2 Mr. Alkhamis Pi-shaped optimized antenna

	Size (mm)
Dipole length	121
Dipole gap	3.8
Feed line width	2.2
Feed line gap	3
Substrate length	246.98
Substrate width	47.38
Substrate thickness	1.27
Pi-end length	25
Pi-end width	18.4

Table I.1. Optimized pi-shaped antenna sizes

This model, with this size and materials, is the model used in all the simulations done in this project.

1.7 Main Goals

The main goal in this project is to study deeply the effects of this antenna in the work frequencies on human body tissues and to find out if this antenna could be considered dangerous or not.

To do that, HFSS software has been used, which provides a SAR calculator and allows us to know how this antenna affects to different human tissues.

Mr. Alkhamis, in his thesis, he simulated a wrist and the wrapped antenna and found out that the SAR levels were not even close to the limits [14].

But the analysis of radiation effects of this antenna can be deeper. First of all, it is possible to simulate a larger arm, to see if it would affect to the parts that are not touching the antenna.

In addition, the wearable wrist antenna will be close to other parts of the body too. It would be interesting to know how the radiation of this antenna could affect, for instance, to human head, when the antenna is close to it.

In conclusion, the goal of this project is to study the radiation of this antenna in human tissues deeply and also that all the work done in this project, afterward, can be useful to analyze radiation effects of other kinds of antennas.

II. HFSS. First simulations and SAR calculations

This chapter contains the explanation of the first simulations done with HFSS. The pi-shaped antenna designed by Mr. Alkhamis has been reproduced and simulated and the first simulations related with SAR have been done.

2.1 Pi-shaped antenna in HFSS

The first step of this project has been to understand and to learn how to use HFSS. In order to do that, some tutorials have been followed [15] [16] [17] [18]. First of all, simple dipoles and micro-strip antenna were designed. It has been also learned how to re-size a design, duplicate objects, and finally how to create excitations and boundaries in order to do a simulation of an antenna in a desired frequency or to sweep a frequency range. Figure 2.1 shows one of the antennas designed in order to learn how HFSS works.

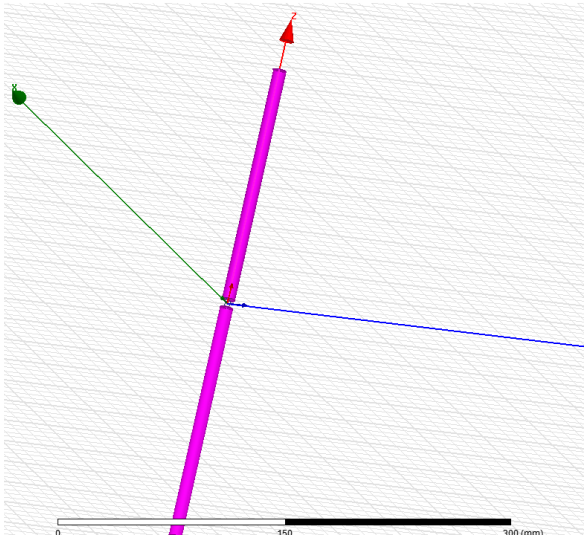

Figure II.1 Example of dipole λ/4 at designed in HFSS

Once used to HFSS and the simulations, the next step has been to reproduce the pi-shape antenna designed by Mr. Alkhamis. This antenna has been designed with copper and with a Duroid Rogers substrate following the sizes of the optimized design of the antenna. In Figure 2.2, it can be seen the design of the planar pi-shaped antenna.

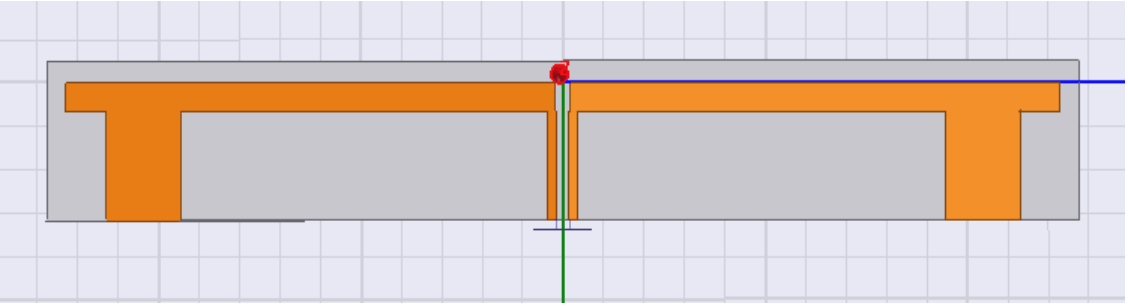

Figure II.2 Design of optimized pi-shaped antenna in HFSS

In Figure 2.3, it can be observed the S_{11} parameter. It can be seen how the antenna is dual-band.

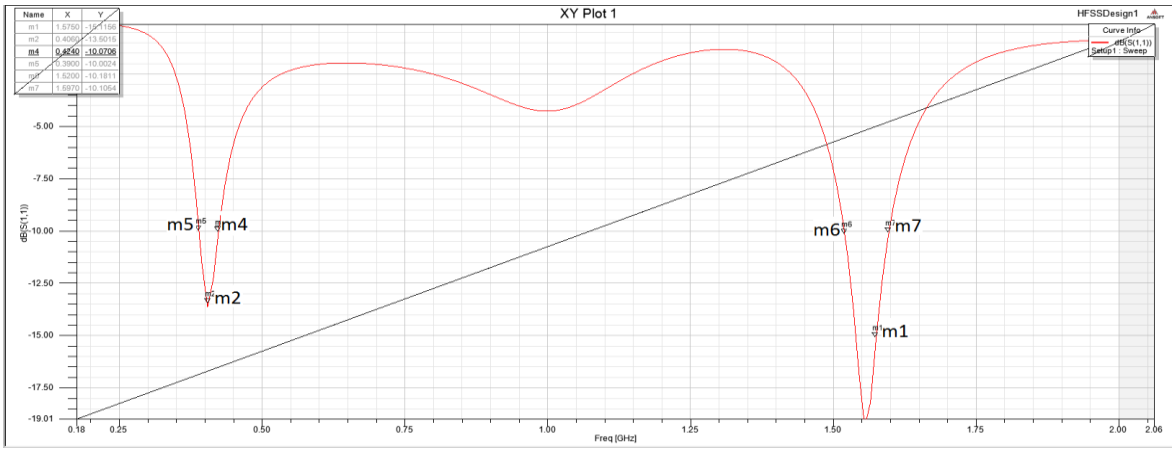

Figure II.3 S_{11} parameter of optimized pi-shaped antenna

In Table 2.1, in can be seen the markers values of Figure 2.3. It can be seen how at the distress frequency (406 MHz) the S_{11} is -13.5 dB. It can also be seen that the bandwidth at this frequency is 34 MHz (marker 4 minus marker 5).

Name	X	Y
m1	1.5750	-15.1156
m2	0.4060	-13.5015
m4	**0.4240**	**-10.0706**
m5	0.3900	-10.0024
m6	1.5200	-10.1811
m7	1.5970	-10.1054

Table II.1 S_{11} values and bandwidth in working frequencies

At the GPS frequency, the value of S_{11} is -15.12 dB and the bandwidth in this case is 77 MHz (marker 7 minus marker 8).

Finally, the radiation patter of rE and the 3D Plot of the realized Gain are presented for the distress signal frequency (406 MHz) in Figures 2.4 and 2.5. It can be seen that the results are the expected and comparing it with [14] it can be concluded that the antenna reproduction has been correctly designed for the 406 MHz work frequency.

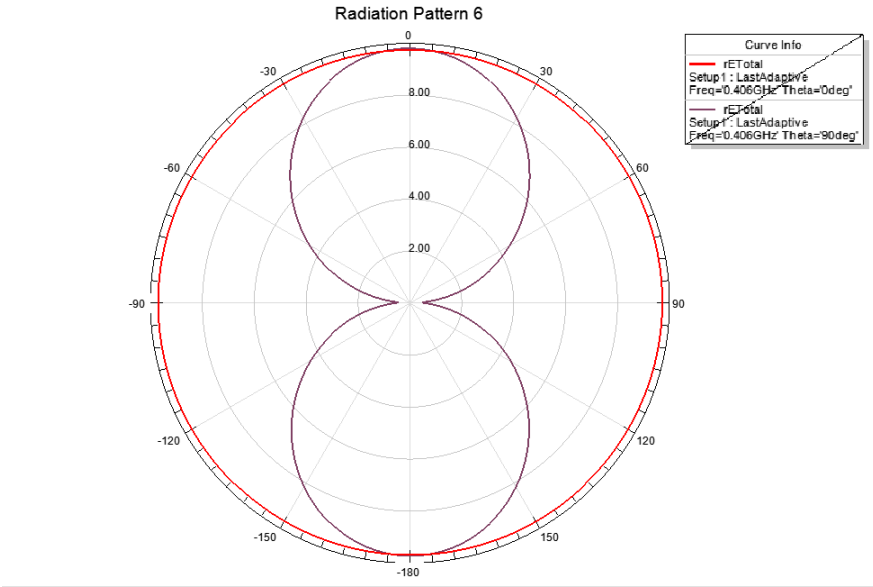

Figure II.4 Radiation pattern of rE at 406MHz

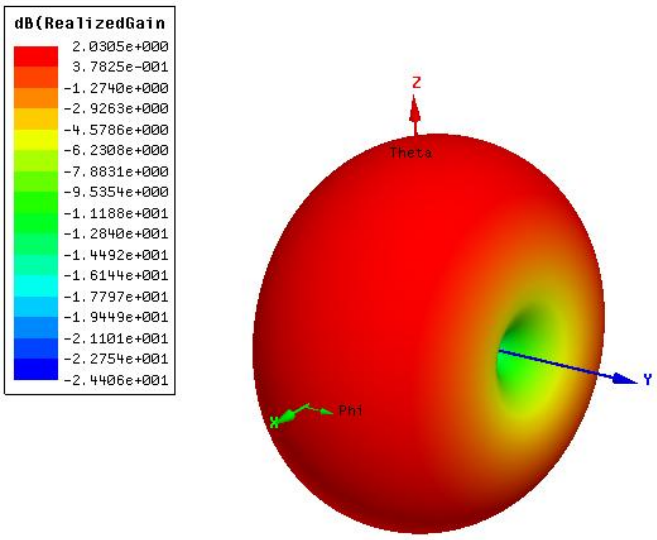

Figure II.5 3D plot of realized gain of the antenna at 406 MHz

The same happens in the GPS frequency. In Figures 2.6 and 2.7 it can be observed the radiation pattern and the 3D plot. As it happened before, if these results are compared

with [14] it can be concluded that the antenna reproduced works equal that the one designed by Mr. Alkhamis.

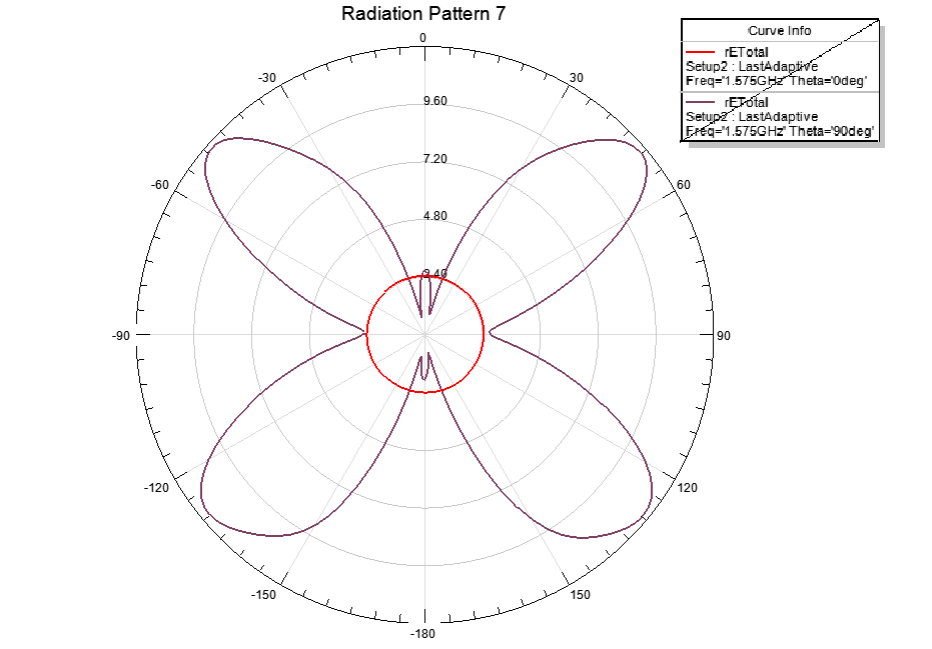

Figure II.6 Radiation pattern of rE at 1575MHz

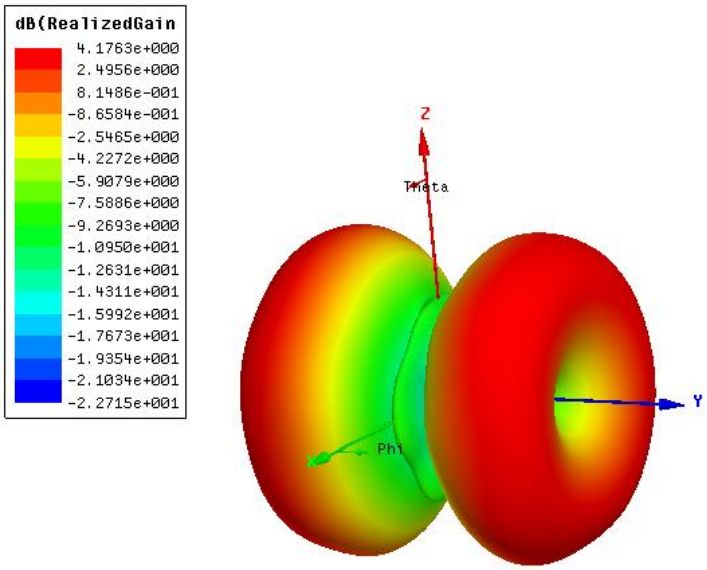

Figure II.7 3D plot of realized gain of the antenna at 1575MHz

2.2 SAR simulations in HFSS

As explained before, HFSS software provides a SAR calculator. It makes possible to know the local and the average SAR in different volumes of the antenna design. Thus, it is possible to create a volume with different layers that represents some part of human body. To do that, the most important thing is to know the characteristics of the different body layers which will represent the different human tissues of that part of the body.

Mr. Alkhamis did some simulations related with SAR levels and concluded that the SAR levels obtained were safe [14]. He focused on the wrist. He represented a 6 layers wrist with 6 different tissues: bone, muscle, blood, nerves, fat and skin.

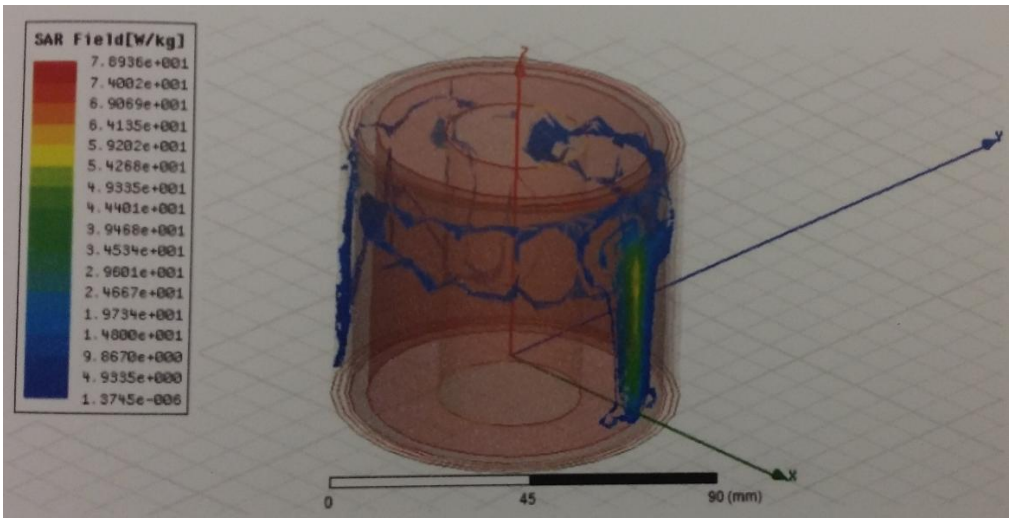

Figure II.8 SAR simulation at 406MHz of wrist done by Mr. Alkhamis.

The first step related with HFSS SAR calculator has been to learn how it works and do some easy simulations. To do that, a tutorial about SAR has been followed [19].

The first simulation done was a simple dipole close to a sphere of two layers. That sphere represents the human head. The two different layers designed simulate the bone layer and, inside, the brain.

To do that, first of all the dipole was designed in HFSS. By creating a cylinder and then duplicate it, the dipole was obtained. Instead of doing it with the size that appear in the tutorial, the size of a dipole chosen has been exactly the size of a dipole which resounds at 406MHz.

Then, a rectangular feeding sheet was placed between the two cylinders. After that, the head was designed. First of all a simple sphere that represented the bone layer was created. Then, the cylinder was opened (using the option “Split” in HFSS). Next, a second sphere, the brain fluid, was created. In order to empty the first sphere and fill it with the second one, both spheres were selected and the option “Substrate” was applied. The last design step was to open the second layer, by using the option “Split” in the second sphere.

Before starting the simulation, the boundary volume was defined and the working frequency was set up at 0.406GHz. Then, the simulation was run. Once, the simulation finished, is when the Local SAR and the Average SAR could be obtained.

At this point, a volume has to be chosen (or a plane as, for instance, XY) and then go to “HFSS/Fields/Other/Average SAR”. Choosing a volume or a plane, the SAR value in this volume is calculated. In Figures 2.9 and 2.10 it can be seen the SAR results obtained for this dipole working at 0.406 GHz with a feed power of 5W.

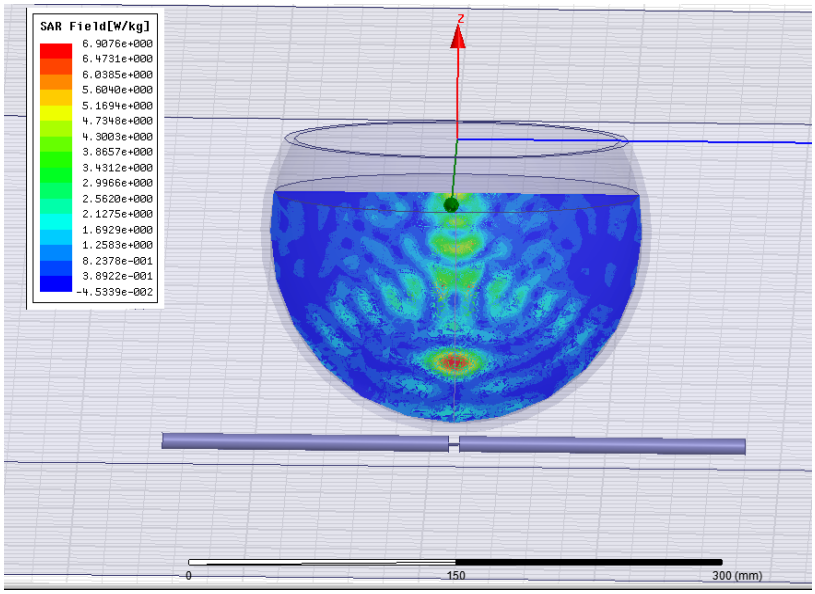

Figure II.9 Average SAR of brain layer in plane YZ of the half-wave dipole at 406MHz

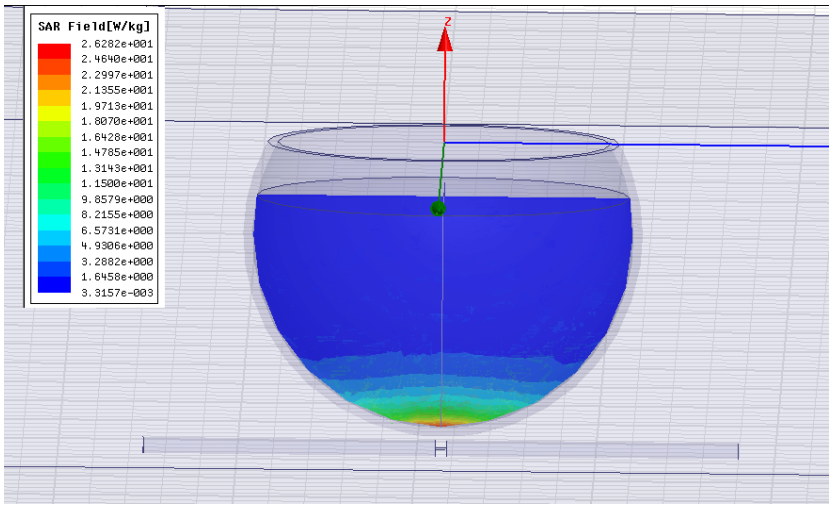

Figure II.10 Local SAR of brain layer in plane YZ of the half-wave dipole at 406 MHz

Finally, a graph of SAR value versus distance can be plotted. To obtain it, before starting the simulation, a line across the volume has to be created. Then, once the simulation has ended, it is possible to obtain a graph of the SAR value (Local and Average) in all the line defined. In the case of the dipole and the two layer head, the line was placed in the Z axis crossing the spheres. The result obtained is in Figure 2.11, where it can be seen the Local SAR and the average SAR in all the line.

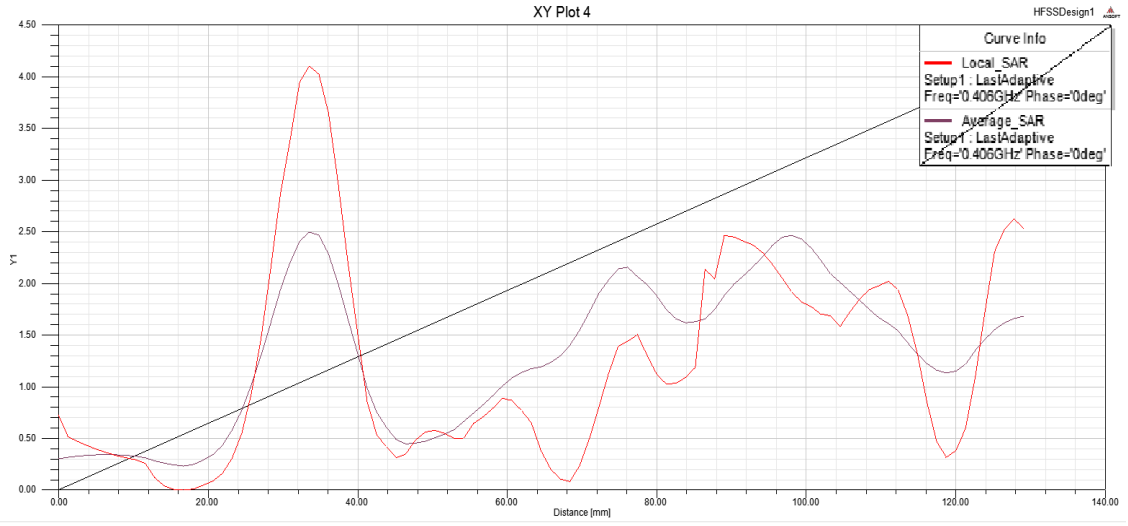

Figure II.11 Comparison between Average SAR and Local SAR in the line crossing the spheres

It must be said that this first simulation was useful to understand how HFSS calculates SAR and to start with a simple design. The Figures presented help to understand the design done but the SAR values are not trustable in this first simulation.

The SAR results obtained here are not relevant because the tissues characteristics were not defined accurately. In addition, head has more layers and it cannot be concluded anything clear about the SAR results obtained in this first simulation.

III. Design of human body parts

The main goal of this project is to study the radiation effect of the dual band pi-shaped antenna deeply. To do that three different configurations of human parts and antenna are presented in this project. This chapter explains the different human parts designed in HFSS and the procedure followed in each case.

3.1 The arm

The wrist and the arm are the body parts closer to the wrapped antenna. They are almost touching the wrapped antenna. The arm might be the body part most affected by the antenna radiation, regarding the short distance between arm tissues and the EM fields. For this reason arm has been the first body part simulated in this project.

Arm is a complex part of body to simulate because it has multiple layers of different tissues. Figure 3.1 shows the complexity of the human arm. Skin, fat, bone, muscle, nerves, blood and arteries are some of the tissues contained in a human arm.

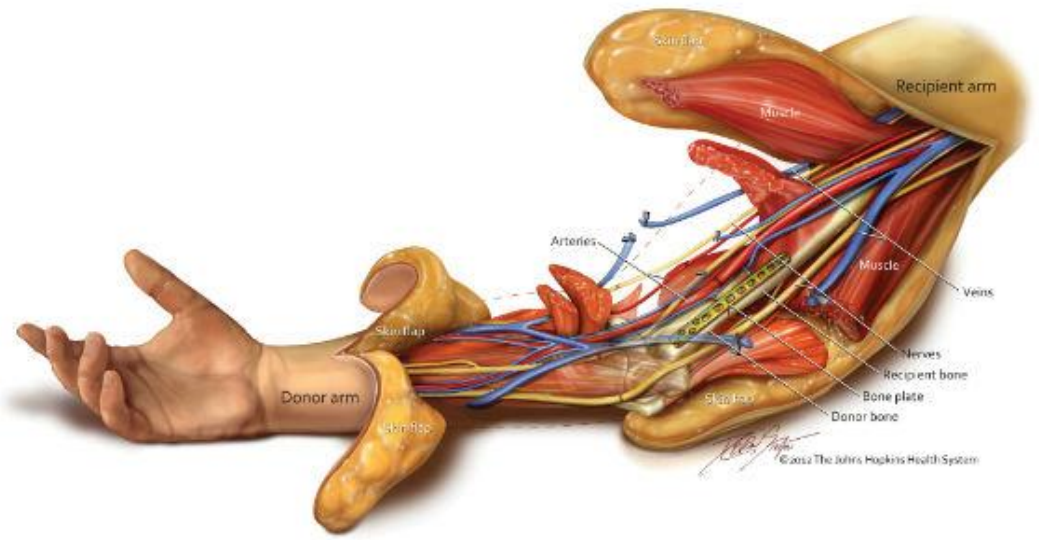

Figure III.1 Picture of arms with different layers by [20]

Regarding the SAR simulations are done in HFSS, it has been necessary to find an HFSS 3D model that represents the wrist. In the SAR simulation done by Mr. Alkhamis in [14], he designed a 6-layers cylinder in which each layer represented one different

tissue. Thus, following the work done by Mr. Alkamis, a very similar 6-layers arm model has been used to simulate the SAR effects in arm.

The 6-layer arm used in this project includes skin tissue, fat tissue, nerves tissue, muscle tissue, blood tissue and bone tissue. The arm model designed is quite longer than the arm presented in Mr. Alkhamis' thesis. This has been done because it can also be interesting to know how the radiation affects to a part of the arm which is not directly touching the wrapped pi-shaped antenna, but really close to it.

The arm model presented and used in the SAR simulations can be observed in Figures 3.2 and 3.3. The total radius of the cylindrical arm model is 41mm and the total high is 116.7 mm. The pi-shaped antenna is placed wrapped around the arm model. The radius of the wrapped antenna is 43.5 mm.

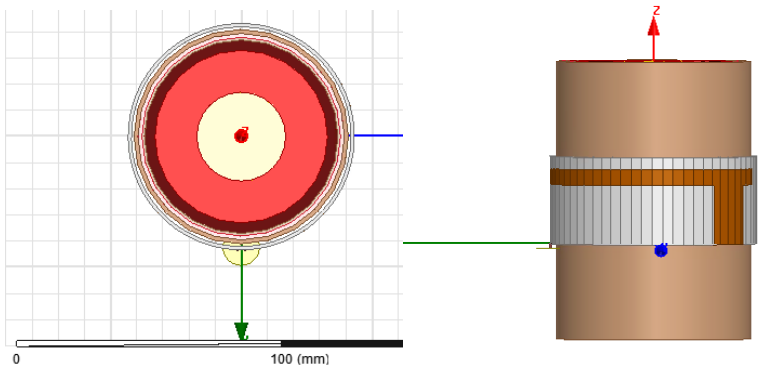

Figure III.2 6-layers arm model in XY plane (left) and XZ plane (right)

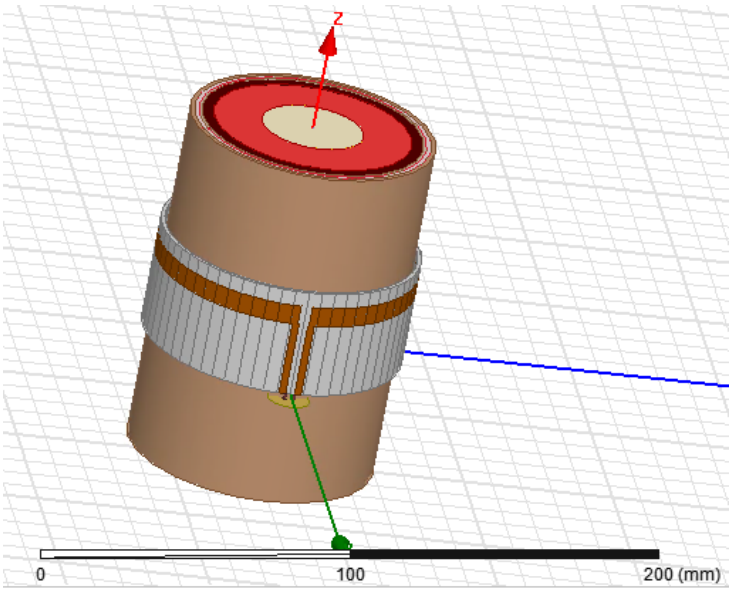

Figure III.3 6-layers arm model in 3D view

Once defined the 3D model arm, it is necessary to define the characteristics of the different arm tissues in HFSS. HFSS requires the mass density, the conductivity, the relative permittivity and the loss tangent of each of the tissues. It has been possible to obtain them using an on-line website which calculates tissues characteristics [21]. This web-site provides the tissues parameters for all the frequency range. Besides, the mass density and the thickness have been obtained from Mr. Alkhamis' thesis [14] and are presented in Table 3.1.

Tissue	Mass densitiy [kg/m3]	Thickness [mm]
Bone	1908	17
Blood	1050	4
Nerve	1075	1
Muscle	1090	15
Fat	911	1.5
Skin	1109	1.5

Table III.1 Arm tissues mass density and thickness [14]

The other tissues characteristics are presented in Tables 3.2 and 3.3 for the two different frequencies of the dual-band antenna, the distress message frequency (406 MHz) and GPS frequency (1575MHz).

Tissue	Conductivity [S/m]	Relative Permittivity	Loss tangent
Bone	0.029385	5.6689	0.22947
Blood	1.3516	64.115	0.93324
Nerve	0.44832	35.339	0.56161
Muscle	0.79787	57.079	0.6188
Fat	0.041216	5.5773	0.32715
Skin	0.69064	46.649	0.65541

Table III.2 Arm tissues parameters at distress signal frequency (406MHz)

Tissue	Conductivity [S/m]	Relative Permittivity	Loss tangent
Bone	0.060428	5.998	0.12769
Blood	1.8962	59.784	0.3169
Nerve	0.76825	31.169	0.28123
Muscle	1.2246	53.855	0.25945
Fat	0.070523	5.3746	0.14972
Skin	1.0992	39.277	0.31933

Table III.3 Arm tissues parameters at GPS frequency (1575MHz)

3.2 The head

The second body part studied and designed in this project is the head and its tissues. The head is the most important body part regarding it contains the most important organ, brain.

Several projects and papers related with the radiation effects of high-frequency EM in head tissue have been done in the past. The main goal of this section is to see how the wearable pi-shaped antenna affects to the head tissues if the antenna is placed close to head.

[22] and [23] study deeply the effect of mobile phones in head tissues. Both of them present exhaustive SAR calculations and simulations using finite-difference time-domain (FDTD) numerical electromagnetic method which has previously been used for bio-electromagnetic problems pertaining to or near-field exposures from ELF to microwave frequencies. These two papers simulate and measure at 900MHz and 1800MHz, so the results found cannot be useful to compare them with the working frequencies of the wearable dual-band antenna. Both papers design the head model with at least two different layers and finding the parameters of the different tissues, then they can obtain the SAR levels in each layer. However, even they are really interesting; none of them use the 3D basic modeling that is available in HFSS Software.

In order to design a head model, it is necessary to know the number of layers and tissues contained on it. Figure 3.4 shows the basic layers of head. Thus, the head model designed should have, at least, the same number of layers.

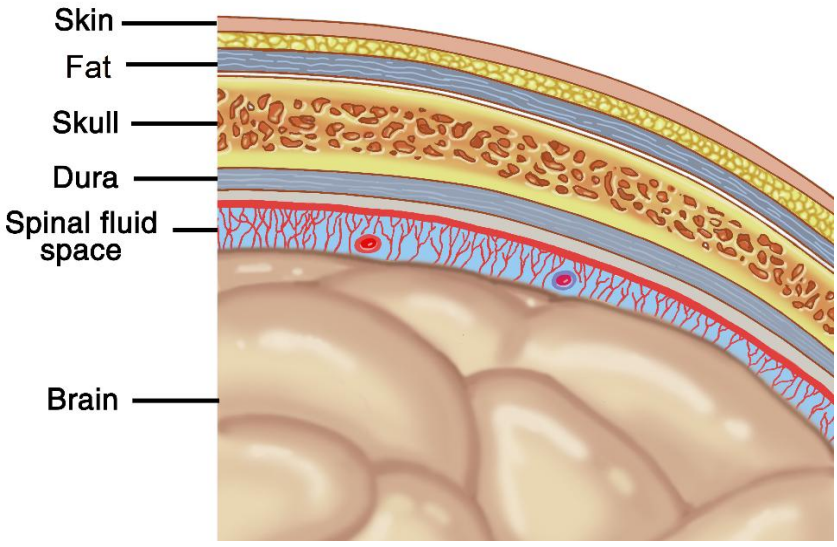

Figure III.4 Layers of human head by [24]

In [24], a paper called “Evaluation of SAR Distribution in Six-Layer Human Head Model”, HFSS software is used in order to design a six-layer head and then simulate the SAR levels with a dipole and a PIFA antenna close to the head model.

The human head design of [24] is done with spheres (3D form available in HFSS) in order to create the head model. The six-layer head is composed by skin, fat, bone, dura, cerebrospinal fluid (CSF) and brain. In Section 2.2 it has been learned how to create a spherical model. In addition, in [24] the model designed contains the same layers that in Figure 3.4. For these reasons, it has been decided to reproduce the same 3D spherical model to obtain the head model of this project.

To create the six-layer head model in HFSS, the procedure followed has been the same that in Section 2.2, but with six layers of six different head tissues. In Figure 3.5, it can be observed the six different spheres designed. Figure 3.6 shows the final head model after putting all the layers together.

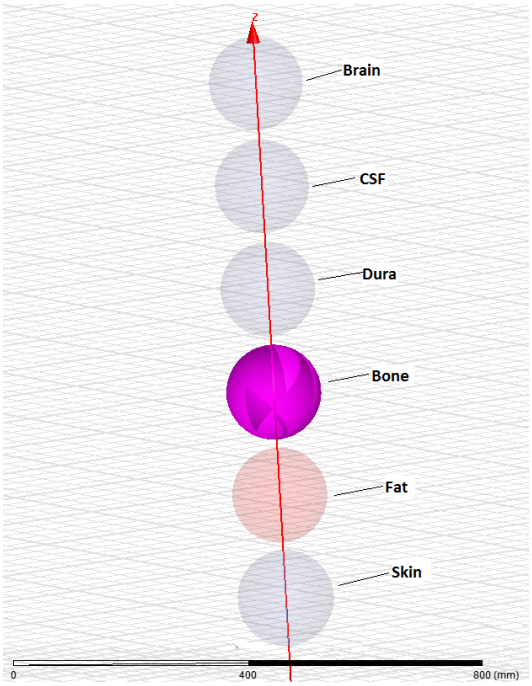

Figure III.5 Six spheres of the six-layer head model

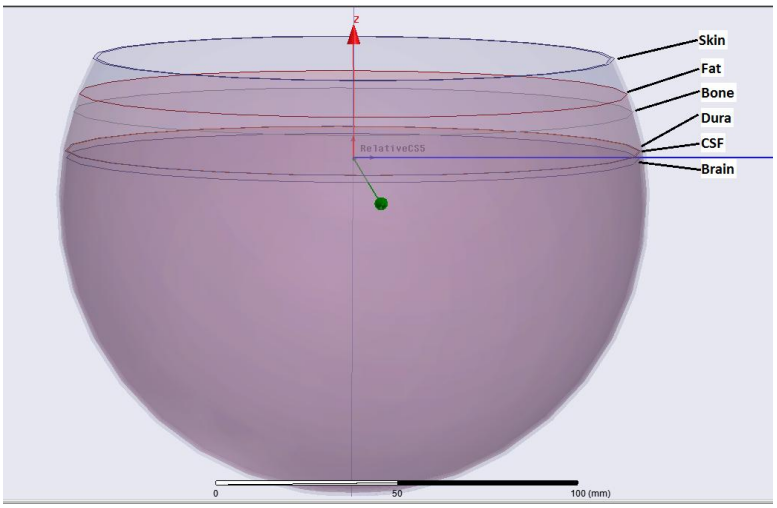

Figure III.6 Final 3D head model designed in HFSS

The next step of the design has been to include the wrapped antenna and put it close to the head model. The antenna is exactly the same that was used for the arm simulations. The substrate cylinder radius of the antenna is 43.5mm and it has been placed close to the head model, at 16.5mm from head. Figures 3.7 and 3.8 show the final design of the head model next to the pi-shaped antenna.

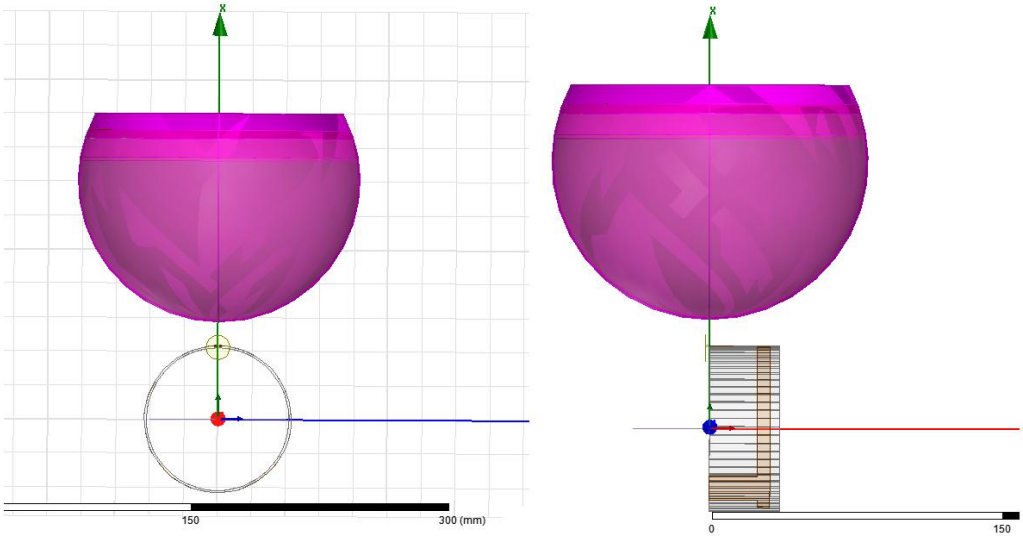

Figure III.7 . 6-layers head model in XY plane (left) and XZ plane (right)

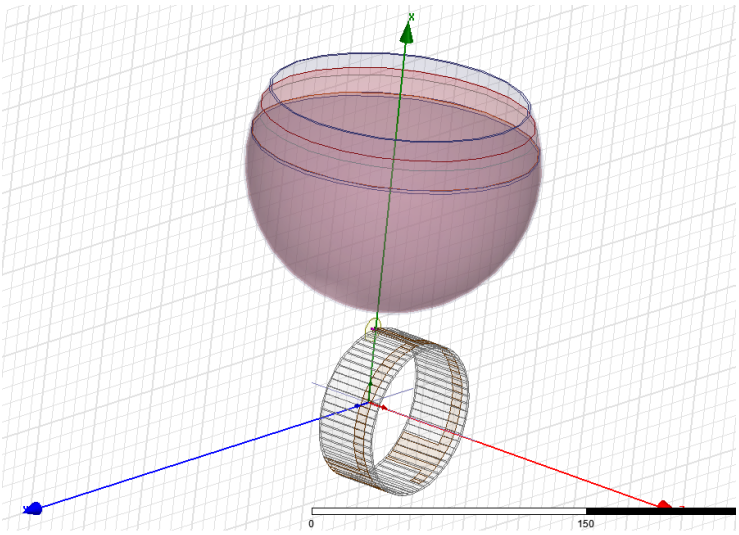

Figure III.8 6-layers head model in 3D view

Once the design has been finished, the next step has been to define the head tissues. As it happened with the arm tissues, [21] has been used to find the parameters. Table 3.4 shows the mass density and the thickness of the six head tissues. Tables 3.5 and 3.6 show the other parameters (conductivity, dielectric permittivity and loss tangent) for the two working frequencies, 406MHz and 1575MHz. After defining these parameters the HFSS head design is finished.

Tissue	Mass density [kg/m3]	Thickness [mm]
Brain	1046	81
CSF	1007	0.2
Dura	1174	0.5
Bone	1908	0.41
Fat	911	0.14
Skin	1109	1

Table III.4 Head tissues mass density and thickness [14]

Tissue	Conductivity [S/m]	Relative Permittivity	Loss tangent
Brain	0.74004	57.319	0.57163
CSF	2.2528	70.927	1.4062
Dura	0.82865	46.61	0.78713
Bone	0.091869	13.133	0.30971
Fat	0.041215	5.5773	0.32718
Skin	0.69062	46.65	0.65546

Table III.5 Head tissues parameters at distress signal frequency (406MHz)

Tissue	Conductivity [S/m]	Relative Permittivity	Loss tangent
Brain	1.2654	50.563	0.28562
CSF	2.7697	67.527	0.46812
Dura	1.2158	43.214	0.32111
Bone	0.23818	11.929	0.22786
Fat	0.070509	5.3747	0.14972
Skin	1.0991	39.278	0.31936

Table III.6 Head tissues parameters at GPS frequency (1575MHz)

3.3. Arm and head

The last HFSS simulations, related with SAR, done during this project have been about the arm tissues and the head tissues together. To do that, the designs of Arm and Head designed before have been put together in the same HFSS design and then the antenna has been wrapped to the arm. The size of the arm and head and the distance between head and the antenna are exactly the same than before.

The main goal of simulating both parts of the body together, which is actually the real case, is to see if the SAR results might change.

The design of this configuration, as explained, is the 6-layers arm with the optimized dual-band antenna wrapped to the arm and the 6 layers head close to the antenna. The main characteristics of the design are:

- Six-layers head: Skin, fat, bone, Dura, Cerebrospinal Fluid, Brain
- Six-layers arm: Skin, fat, muscles, nerves, blood, bone
- Optimized Pi-Shaped Antenna in Rogers Substrate
- Substrate cylinder radius: 43.5 mm
- Skull radius: 85mm
- Wrist radius: 41 mm
- Wrist length: 116.7 mm
- Distance between antenna and Brain: 16.5 mm

The design of the HFSS configuration can be seen in Figures 3.9 and 3.10. In these figures it can be observed the 6-layers arm (pink) and the 6-layers head (brown). In Figure 3.11 it can be observed the wrapped antenna around the arm.

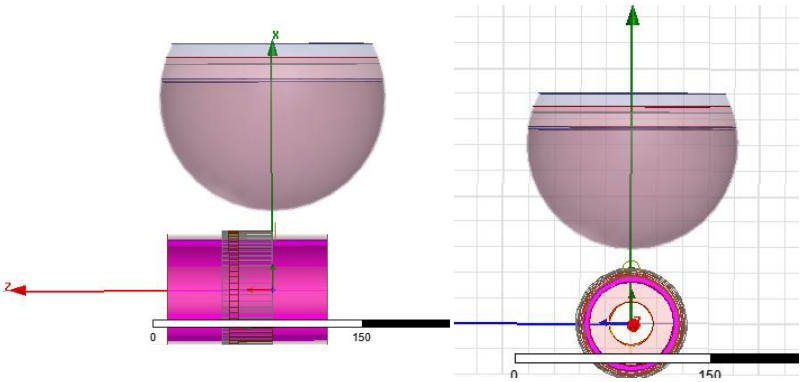

Figure III.9 HFSS design of arm, head and antenna in XZ plane (left) and in XY plane (right)

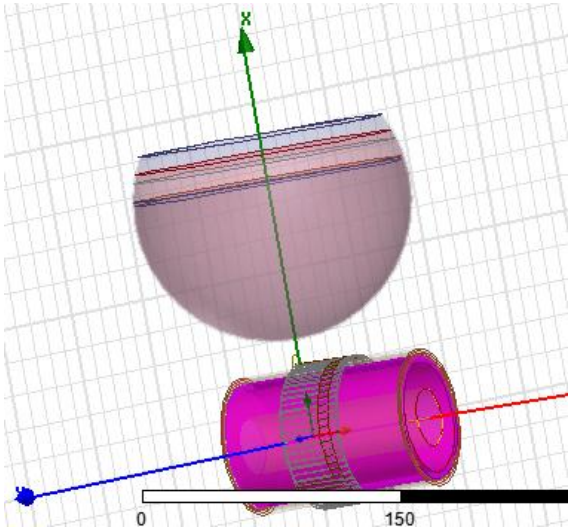

Figure III.10 HFSS design of arm, head and antenna in 3D view

IV. Results I. SAR HFSS Results

This chapter presents the results of the SAR simulations done with three different configurations of body parts. Average and local SAR results are presented for all the body tissues designed in Chapter 3.

4.1 Arm tissues SAR Results

With the model of the arm defined, the next step has been to simulate the antenna radiation at the two antenna working frequencies. First of all, the source has been set to 5 W (transmitting power) and the frequency has been set at 406MHz (transmitting frequency).

After finishing the 406MHz simulation, the local and average SAR have been calculated with HFSS SAR calculator. Figure 4.1 shows an example of the average SAR results obtained in skin tissue at 406MHz. All the SAR results obtained at the distress signal frequency are presented in Table 4.1.

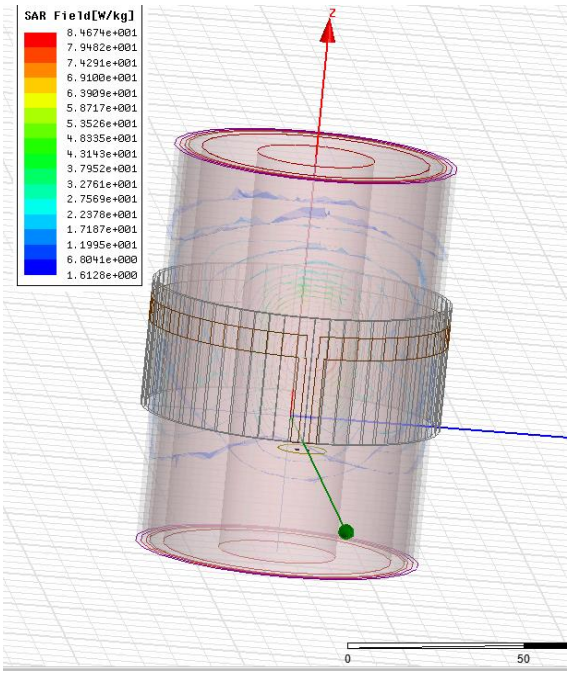

Figure IV.1 Average SAR in skin tissue at 406MHz

Tissue	Average SAR (W/kg)	Local SAR (W/kg)
Bone	0.0172	0.024345
Blood	0.678	6.531
Nerve	10.175	81.674
Muscle	18.318	19.571
Fat	0.5967	1.264
Skin	**84.674**	**319.22**

Table IV.1 Average and local SAR results at 406MHz and 5 W

Regarding the SAR results obtained, it can be concluded that the most affected tissue is, without any doubt, the skin. It can be observed that the levels of local SAR (single point of tissue) are higher than the average SAR (averaging the tissue volume). In addition, there are 3 tissues with an average SAR clearly above the SAR limit in USA (1.6 W/kg). Nerve, muscle and skin are above the SAR limit and the value of average skin SAR is really high compared with SAR U.S. limit.

Even though, the high SAR levels are not enough to conclude if the antenna may be dangerous for human. Even if the SAR results are really high is it also necessary to know other parameters like the time of exposure of the tissues to the EM fields of the antenna.

The same procedure has been followed to simulate the GPS frequency. The source power, in this case, has been set to 1mW and the frequency at 1575MHz. Once the simulation finished, the SAR values have been calculated too (Table 4.2).

Tissue	Average SAR (W/kg)	Local SAR (W/kg)
Bone	1.76E-03	3.25E-03
Blood	5.49E-03	9.73E-03
Nerve	5.71E-04	2.35E-03
Muscle	2.61E-03	5.91E-03
Fat	**7.29E-03**	3.30E-03
Skin	1.27E-03	**6.01E-02**

Table IV.2 Average and local SAR results at 1575MHz and 1mW

At the GSP frequency, due to the frequency and to the small power, the SAR levels are lower than the levels obtained at 406MHz. None of the average SAR results are above the SAR U.S. limit. All of them are clearly below the limit for the pi-shaped antenna receiving GPS signals. Besides, regarding average SAR results, at 1575MHz the most affected tissue is the fat. Regarding local SAR, the most affected tissue is skin.

4.2 Head tissues SAR results

The head model has been simulated at the two working frequencies of the dual-band pi-shaped antenna.

Then, the SAR calculator has been used in order to find the local SAR and the average SAR of the head tissues. In Figure 4.2 it can be observed one of the average SAR calculations done. The final results of local and average SAR can be seen in Table 4.3 and Table 4.4.

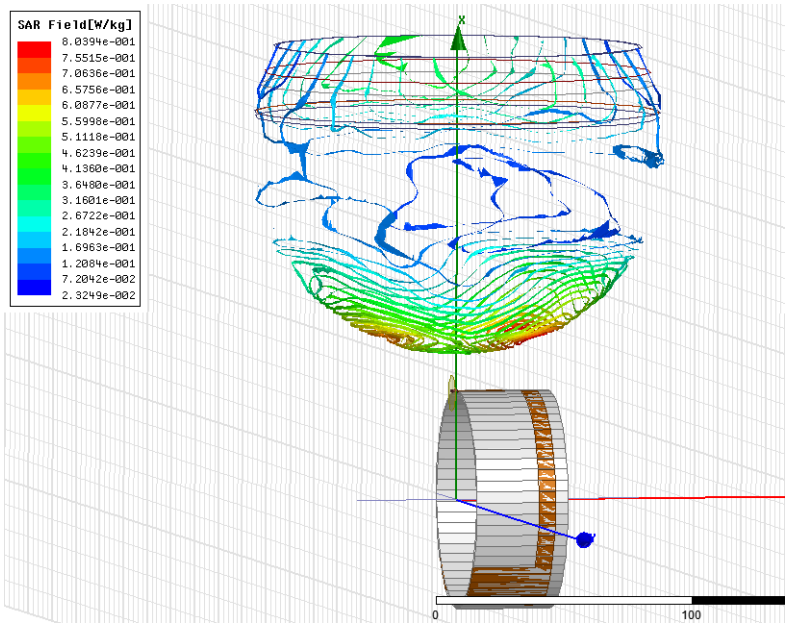

Figure IV.2 Average SAR in skin head tissue at 406MHz

Tissue	Average SAR (W/kg)	Local SAR (W/kg)
Brain	2.554	4.912
CSF	13.081	3.65E+01
Dura	6.59E-01	3.87E+01
Bone	6.48E-03	3.24E-01
Fat	6.38E-03	5.25E-01
Skin	8.04E-01	6.36E+02

Table IV.3 Average and local SAR results at 406MHz and 5 W

In table 4.3 can be observed that the most affected tissue is the cerebrospinal fluid in the case of the average SAR. Its value is above the average SAR U.S. limit. In addition,

at 406MHz, brain tissue has also a value of average SAR above the U.S. limit. For local SAR, the highest level appears in skin where there is a single point in this tissue with a really high value of SAR, 636 W/kg. Even though, as it was mentioned in the previous section, only with the SAR values, is not possible to conclude if the antenna could be dangerous for human use.

Tissue	Average SAR (W/kg)	Local SAR (W/kg)
Brain	5.32E-04	2.45E-03
CSF	3.02E-03	3.67E-02
Dura	1.13E-04	6.30E-03
Bone	3.71E-05	5.13E-03
Fat	1.74E-05	3.14E-04
Skin	7.67E-06	**3.02E-03**

Table IV.4 Average and local SAR results at 1575MHz and 1mW

For the GPS frequency, the most affected tissue is CSF, with an average SAR value of 3.02mW/kg and a local SAR value of 36.7mW/kg. At his frequency and power source, all the SAR levels of the six head tissues are not relevant. All of them are much lower that in the 406MHz and they are far from the SAR limits.

4.3 Head and Arm tissues together SAR results

For the arm and the head configuration put together, the design has been simulated at 406MHz and 5 W (transmitting frequency and feed power). It has taken a long time to complete this simulation with HFSS, due to the complex tissues and antenna volumes and forms and also because of the amount of different tissues with different characteristics.

After the simulation, it has been possible to obtain the local and average SAR values. For 406MHz and 5W, the SAR results in the twelve different tissues are presented in Table 4.5.

Tissue	Average SAR (W/kg)	Local SAR (W/kg)
Brain	2.43E-01	4.523
CSF	**1.1427**	3.8099
Dura	7.64E-02	5.4179
Bone	2.85E-03	4.94E-01
Fat	2.75E-03	1.21E-01
Skin	9.41E-02	4.52E-01
Bone	1.68E-02	2.95E-02
Blood	6.50E-01	7.52E+00
Nerve	**9.80E+00**	1.16E+02
Muscle	**1.75E+01**	1.94E+01
Fat	6.28E-01	1.54E+00
Skin	**8.14E+01**	3.51E+02

Table IV.5 Average and Local SAR values in arm and head tissues at 406MHz and 5 W

Regarding Table 4.5, the highest value of Average SAR is 81.4 W/kg and the highest value of Local SAR is 351 W/kg. Both values are from arm skin tissue. It means that skin of arm is the most affected tissue, as it could be expected (Section 4.1). Nerves and fat of arm are also highly affected and have average SAR levels above the U.S.A limit (1.6 W/kg).

The most affected head tissue is CSF with 1.14 W/kg of average SAR. In general, arm tissues, which are touching the wrapped antenna, have higher SAR values than head tissues. The only exception is Cerebrospinal fluid, with an average SAR level higher than blood of arm and fat of arm.

In order to see if the SAR results of head and arm together are different than the ones obtained simulating arm and head separately, a comparison has been done. Tables 4.6 and 4.7 show the SAR results obtained in the last simulation (arm and head together) and the results obtained simulating them separately (Sections 4.1 and 4.2).

Tissue	Together Average SAR (W/kg)	Separately Average SAR (W/kg)	Difference SAR (W/kg)
Brain	0.2429	2.554	2.3111
CSF	1.1427	13.081	11.9383
Dura	0.0764	0.6587	0.582275
Bone head	0.0029	0.0065	0.0036303
Fat head	0.0028	0.0064	0.003627
Skin head	0.0941	0.8039	0.709832
Bone arm	0.0168	0.0172	0.0004
Blood	0.6496	0.678	0.02839
Nerve	9.8003	10.175	0.3747
Muscle	17.54	18.318	0.778
Fat arm	0.6284	0.5967	0.03172
Skin arm	81.368	84.674	3.306

Table IV.6 Average SAR levels in the 12 body tissues for Arm and head together and separately and difference

Tissue	Together Local SAR (W/kg)	Separately Local SAR (W/kg)	Difference SAR (W/kg)
Brain	4.523	4.912	0.389
CSF	3.8099	3.65E+01	32.7331
Dura	5.4179	3.87E+01	33.2921
Bone head	4.94E-01	3.24E-01	0.16918
Fat head	1.21E-01	5.25E-01	0.40371
Skin head	4.52E-01	6.36E+02	635.5477
Bone arm	2.95E-02	0.024345	0.00519
Blood	7.52E+00	6.531	0.9931
Nerve	1.16E+02	81.674	34.226
Muscle	1.94E+01	19.571	0.214
Fat arm	1.54E+00	1.264	0.2756
Skin arm	3.51E+02	319.22	31.71

Table IV.7 Local SAR levels in the 12 body tissues for Arm and head together and separately and difference

In Tables 4.6 and 4.7 the second column is the value of SAR (average or local) obtained in last simulation (arm and head). The third column is the SAR levels obtained simulating each body part separately (Sections 4.1 and 4.2). Finally, the fourth column shows the difference between the second and the third column. In both tables, the SAR difference higher than 1 W/kg has been marked in red.

In Table 4.6 it can be observed that all the average SAR levels except one (fat of arm), are lower when arm and head are simulated together than when they are simulated

separately. In addition, for the average SAR the differences are not very high. Only three tissues, brain, CSF and arm skin have differences above 1 W/kg. The highest average SAR difference is in cerebrospinal fluid, with a difference of 11.93 W/kg between the arm and head simulated together and separately.

Table 4.7 shows the local SAR levels and the differences between the two simulations. In this case the differences are higher. There are five tissues with a difference higher than 1 W/kg (CSF, dura, skin head, nerve and skin arm). Besides, the highest difference appears in skin of head. The difference of local SAR between both simulations in this case is really high, 635.54 W/kg.

In conclusion, average SAR levels are, in general, lower when arm and head are simulated together than when they are simulated separately. Average SAR differences between both simulations are not really big (11.93 is the highest average SAR difference). In case of local SAR, the results are quite different for both simulations and the highest difference is more than 635 W/kg.

After analyzing these results, and regarding that the simulations conditions were exactly the same, it can be said that the SAR results change if two body parts are simulated together or if they are simulated and analyzed separately.

V. Results II. Increase of temperature

This chapter presents, for the body parts simulated in Chapter 3, results related with the temperature increase of the human tissues due to the EM fields radiated by the wearable antenna.

5.1 Short time of exposure to EM fields

In Section 1.5.1 it has been explained that, in case of short times of exposure of human tissues to high-frequency EM fields, it is possible to find the increase of temperature of tissues using a simple formula which relates average SAR and temperature. This section is about the increase of temperature of tissues in short exposure time to EM high-frequency fields.

5.1.1 Increase of temperature in arm tissues

For arm tissues it has been possible to obtain the increase of temperature during the real transmitting time of the pi-shaped antenna. In [17] is explained that the pi-shaped antenna transmits distress signals of 550ms every 50 seconds. It means that the antenna is transmitting during 550ms.

Using this value of exposure time and finding the heat capacity of arm tissues [26], then it is possible to obtain directly the increase of temperature of the tissues using the formula of Section 1.5.1.

The results presented in this section are at the transmitting frequency (406MHz). In the distress signal frequency is where the SAR levels are high and above the U.S. limit. In addition, at this frequency the time of transmission is known, so it only makes sense to obtain the increase of temperature at this frequency. Besides, it is important to know the increase of temperature when the SAR levels are above the limit, in order to see if it also means a high increase of temperature.

Thus, Table 5.1 shows the heat capacity values of the 6-layers arm tissues, in J/(Kg·K). Table 5.2 shows the increase of temperature calculated using the linear formula, for average SAR and for local SAR.

Tissue	Heat Capacity (J/(Kg·K))
Bone	2065
Blood	3617
Nerve	2613
Muscle	3421
Fat	2348
Skin	3391

Table V.1 Heat capacity of the 6 arm tissues

Tissue	T(average SAR) (K)	T(local SAR) (K)
Bone	4.52785E-06	6.39225E-06
Blood	0.000103096	0.000993102
Nerve	0.002141695	0.017191236
Muscle	0.002945016	0.003146463
Fat	0.000139772	0.000296082
Skin	0.013733618	0.051775582

Table V.2 Increase of temperature of arm tissues at 550ms

Observing the results obtained in Table 5.2, the highest value of temperature increase is found in skin, with less than 0.014 K (using average SAR in the formula). Even regarding local SAR, which is always higher, the highest value for skin is 0.052 K.

Thus, it can be concluded that, for the six arm tissues, the increase of temperature is really small in the real case of 550ms exposure time. It means that, even the SAR levels were above the limits, due to the short time of transmission, the rise of temperatures cannot damaging the arm tissues.

5.1.2 Increase of temperature in head tissues.

As it happened in the case of the arm model, it is interesting to know the increase of temperature of the head tissues. It is necessary to know if the high SAR levels of CSF and brain tissues at 406MHz, in the real exposure time of the pi-shaped antenna transmission, will mean also a high increase of temperature in the head tissues.

To find the increase of temperature in short time exposures it is necessary to know the time of exposure (550ms, [17]) and the heat capacities of the six head tissues (Table 5.3, [3]).Then, the temperature increase has been calculated using the linear formula of Section 5.1.1. The results are presented in Table 5.4.

Tissue	Heat Capacity (J/(Kg·K))
Brain	3583
CSF	4096
Dura	3364
Bone	1313
Fat	2348
Skin	3391

Table V.3 Heat capacity of the 6 head tissues

Tissue	T(average SAR) (K)	T(local SAR) (K)
Brain	0.000392046	0.000754005
CSF	0.001756482	0.004906897
Dura	0.000107695	0.006328924
Bone	2.71607E-06	0.000135887
Fat	1.49399E-06	0.00012293
Skin	0.000130388	0.103155411

Table V.4 Increase of temperature of arm tissues at 550ms

Regarding Table 5.4, it can be concluded that, for the real transmitting time of the wearable pi-shaped antenna, the increase of temperature of all the head tissues are not relevant. Even the highest value of temperature increase, found in a single point of skin tissue, is only 0.103 K.

5.2 Long exposure time to EM fields

5.2.1 Rise of temperature in long time exposure to EM fields

In order to obtain the relation between rise temperature and time, in the case of long time exposures, the Bio Heat Pennes equation has been used. In [27] there is a solution for the equation in case in absence of thermoregulation, and for brain tissues (sphere). It is explained that in case of brain is possible to obtain the maximum rise of temperature and also the rise temperature in function of time.

First of all from the general formula:

$$\rho c \frac{\partial T}{\partial t} = \nabla(k \nabla T) + \rho Q + \rho S - \rho_b c_b \rho \omega (T - T_b)$$

In [27] it is simplified (with no thermoregulation) and presented as:

$$\rho c \frac{\partial T}{\partial t} = k\nabla^2 T + \rho S - Vs(T - T_b)$$

Where in the this equation, $Vs = \rho_b c_b \rho \omega$.

By dividing all the equation by *k*, the equation can be presented like this:

$$\mu \frac{\partial T}{\partial t} = \nabla^2 T + q - \lambda'(T)$$

In the equation, μ is equal to density multiplied by heat capacity and divided by thermal conductivity of tissue, λ' is $\rho_b c_b \rho \omega$ divided by thermal conductivity and q is equal to mass density multiplied by the average SAR value and divided by the thermal conductivity:

$$\mu = \frac{\rho c}{k}, \qquad \lambda' = \frac{Vs}{k}, \qquad q = \frac{\rho S}{k}$$

From this equation [27] obtains the maximum rise of temperature. The equation presented is:

$$T_{max} = \frac{q}{\lambda'}[1 - \left(\sqrt{\lambda'}A + 1\right) e^{-\sqrt{\lambda'}A}]$$

Where A is lambda (in meters) divided by 4 ($A = \frac{\lambda}{4}$).

But the most interesting thing of [27] is the transient case. In order to obtain the time dependency, they use the Fourier Transform, obtaining the formula:

$$\nabla^2 T_\omega - k^2 T_\omega = -q_\omega$$

In this equation, $k^2 = \lambda + i\omega\omega\mu$, T_ω and q_ω are the Fourier Transform of T and q.

Then, they do the inverse Fourier transform and finally they obtain the temperature in time domain. There are two different formulas depending on the radius of the sphere value. It depends if the sphere radius of the head tissue (R) is smaller or bigger than $\frac{\lambda}{4}$ (A).

If $R < A$, the equation is:

$$T_1(t) = \frac{q}{\lambda'}(1 - e^{-\tau}) - \frac{q}{2\lambda'}\frac{\rho}{r}\left\{\frac{e^{-(\rho-r)}}{2}\left(1 + \frac{1}{\rho}\right) \cdot erfc\left(\frac{\rho-r}{2\sqrt{\tau}} - \sqrt{\tau}\right) + \frac{e^{-(\rho-r)}}{2}\left(1 - \frac{1}{\rho}\right) \cdot erfc\left(\frac{\rho-r}{2\sqrt{\tau}} + \sqrt{\tau}\right) - \frac{e^{-(\rho+r)}}{2}\left(1 + \frac{1}{\rho}\right) \cdot erfc\left(\frac{\rho+r}{2\sqrt{\tau}} - \sqrt{\tau}\right) - \frac{e^{(\rho+r)}}{2}\left(1 - \frac{1}{\rho}\right) \cdot erfc\left(\frac{\rho+r}{2\sqrt{\tau}} + \sqrt{\tau}\right) - \frac{r}{\rho}e^{-\tau}\left[erfc\left(\frac{\rho-r}{2\sqrt{\tau}}\right) + erfc\left(\frac{\rho+r}{2\sqrt{\tau}}\right) + \frac{2}{\rho}\sqrt{\frac{\tau}{\pi}}\left(\exp - \frac{(\rho+r)^2}{4\tau} - exp - \frac{(\rho-r)^2}{4\tau}\right)\right]\right\}$$

Otherwise, if $R > A$, the equation is:

$$T_2(t) = \frac{q}{2\lambda'}\frac{\rho}{r}\left\{\frac{e^{(r-\rho)}}{2}\left(1+\frac{1}{\rho}\right)\cdot erfc\left(\frac{r-\rho}{2\sqrt{\tau}}\right) + \frac{e^{-r-\rho}}{2}\left(1-\frac{1}{\rho}\right)\cdot erfc\left(\frac{\rho-r}{2\sqrt{\tau}}-\sqrt{\tau}\right) - \frac{e^{(p+r)}}{2}\left(1-\frac{1}{\rho}\right)\cdot erfc\left(\frac{\rho+r}{2\sqrt{\tau}}+\sqrt{\tau}\right) - \frac{e^{-(r+\rho)}}{2}\left(1+\frac{1}{\rho}\right)\cdot erfc\left(\frac{\rho+r}{2\sqrt{\tau}}-\sqrt{\tau}\right) + \frac{r}{\rho}e^{-\tau}\left[erfc\left(\frac{\rho+r}{2\sqrt{\tau}}\right) + erfc\left(\frac{r-\rho}{2\sqrt{\tau}}\right) + \frac{2}{\rho}\sqrt{\frac{\tau}{\pi}}\left(\exp -\frac{(r-\rho)^2}{4\tau} - exp - \frac{(\rho+r)^2}{4\tau}\right)\right]\right\}$$

In the formulas $T_1(t)$ and $T_2(t)$, the $erfc(x)$ function is defined as $erfc(x) = 1 - erf(x)$.

In mathematics, $erf(x)$ is known as the error function (or Gauss error function. It is a special function of sigmoid shape which occurs in probability, statistics and partial differential equations [20]. It is defined as $erf(x) = \frac{2}{\sqrt{\pi}}\int_0^x e^{-t^2}dt$. Thus, the complementary function, $erfc(x)$, is defined as $1 - \frac{2}{\sqrt{\pi}}\int_0^x e^{-t^2}dt$.

The other parameters of the $T_1(t)$ and $T_2(t)$ formulas are:

$$\rho = \sqrt{\lambda'}A, \qquad \tau = \frac{\lambda'}{\mu}t, \qquad r = \sqrt{\lambda'}R, \qquad erfc(x) = 1 - \frac{2}{\sqrt{\pi}}\int_0^x e^{-t^2}dt$$

$T_1(t)$ and $T_2(t)$ can be really useful to observe what would happen in the worst case of the antenna transmission. The worst case would mean to be transmitting beacons messages of 550ms during 10 minutes, what would mean to be transmitting continuously during 6.6 minutes. If the equation above is plotted, considering the different body tissues and the different parameters, the evolution time of the rise of temperature for long time exposure will be obtained.

5.2.2 Increase of temperature of head tissues

Methodology

The results of this part are about the head tissues and in transmission mode (Beacons at 406 MHz and 5 W). The main reason is that the SAR values (and then the

temperature rises) are higher at this frequency. Also, it is known the time of exposure for transmission, so it is possible to obtain the time evolution and the rise of temperature for the transmission case.

First of all, the maximum temperature rise has been obtained. It means the continuous operation maximum temperature that the tissues could increase if they were exposed to EM fields radiated by the PI- Shaped antenna for infinite time.

To do that, the *Tmax* formula shown before has been used in the 6 different tissues of the human head.

For each of the six tissues it is necessary to know:

- ρ= density of tissue [kg/m^3]
- c= heat capacity of tissue [J/kg/˚C]
- k= thermal conductivity of tissue [W/m/˚C]
- S= Average SAR in the tissue [W/kg]
- ρ_b= density of blood [kg/m^3]
- c_b= heat capacity of blood [kg/m^3]
- ω= blood perfusion rate in brain tissues [ml/g/min] (typically 0.5 – 0.54)

The 6 tissues parameters are shown in Table 5.5. The blood parameters and the blood perfusion rate are presented in Table 5.6. It must be said that the blood perfusion rate is different depending on the part of the body. For brain tissues, blood perfusion rate is typically 0.5 -0.54 ml/g/min.

Tissue	Mass densitiy [kg/m3]	Thermal Conductivity[W/m/˚C]	Heat Capacity [J/kg/˚C]	Average SAR [W/kg]
Brain	1046	0,51	3583	2,554
CSF	1007	0,57	4096	13,081
Dura	1174	0,44	3364	6,59E-01
Bone	1908	0,32	1313	6,48E-03
Fat	911	0,21	2348	6,38E-03
Skin	1109	0,37	3391	8,04E-01

Table V.5 Head Tissues parameters

Tissue	Heat Capacity [J/kg/˚C]	Blood perfusion rate [ml/g/min]	Mass densitiy [kg/m3]
Blood	3617	0.5	1050

Table V.6. Blood perfusion parameters

With these values calculated, now it is possible to obtain T_{max}. The maximum rise of temperature for the 6-layers head brain tissues affected by the pi-shaped EM fields are shown in table 5.7.

	Maximum Temperature Rise (K)
Brain	8,1E-02
CSF	3,70E-01
Dura	2,40E-02
Bone	3,30E-04
Fat	4,90E-04
Skin	3,50E-02

Table V.7 Maximum rise of temperature for head tissues at 406 MHz

The next step has been focused on solving and plotting the transient case equation, *T(t)* also at 406MHz. In this case the equation required is $T_1(t)$. This is because at 406 MHz, $A = \frac{\lambda}{4} = 184.73\ mm$ and the radius of the biggest head sphere (skin tissue, see Table 5.8) is $R = 83.3\ mm$, so it means that r < ρ.

In order to obtain the transient case, $T_1(t)$, a Maltab script has been done. Regarding $T_1(t)$ is a really long and complex formula which includes *erfc(x)* function; Matlab is the most suitable software tool to plot and to solve this equation.

To plot $T_1(t)$, it is necessary to use the parameters of tables 5.5 and 5.6 and also the radius of each sphere tissue (shown in Table 5.8). Then, for each tissue, the same Matlab script has been used, considering the different tissue parameters that appear in the formula $T_1(t)$. In the code below is the Matlab Script with the parameters of Brain tissue.

Tissue	Sphere Radius (mm)
Brain	81
CSF	81,2
Dura	81,7
Bone	82,11
Fat	82,25
Skin	83,25

Table V.8 Sphere radius of six-layers head

```
close all;
t=[0:0.01:1000];
thau=8.83E-03*t;
p=4.71E+01;
lambda=6.49E+04;
mu=7348662.745;
r=2.06E+01;
q=5238.203922;
T=q./lambda.*(1-exp(-thau))-q./(2.*lambda).*p./r.*(exp(-(p-
r))./2.*(1+1./p).*erfc((p-r)./(2.*sqrt(thau))-sqrt(thau))
+exp((p-r))./2.*(1-1./p).*erfc((p-r)./(2.*sqrt(thau))+sqrt(thau))-
exp(-(p+r))./2.*(1+1./p).*erfc((p+r)./(2.*sqrt(thau))-sqrt(thau))
-exp((p+r))./2.*(1-1/p).*erfc((p+r)./(2.*sqrt(thau))+sqrt(thau))-
r./p.*exp(-thau).*(erfc((p-
r)./(2.*sqrt(thau)))+erfc((p+r)./(2.*sqrt(thau))
)+2./p.*sqrt(thau./pi).*(exp(-(p+r)^2./(4.*thau))-exp(-(p-
r)^2./(4.*thau)))));
figure,plot(t,T);
axis([0 1000 0 0.09]);
xlabel('Time(seconds)')
ylabel('Temperature Rise (K)')
title ('Rise of temperature in Brain Head Tissue','FontSize',12)
hold on;
yi = interp1(t,T,396);
plot(396,yi,'r*');
hold on;
yii = interp1(t,T,0.55);
plot(0.55,yii,'b*');
```

Matlab script used to find $T_1(t)$ in brain tissue

Evolution time of temperature increase

Once the script has been run for each tissue, the result is a graph of the time evolution of the temperature increase and also the temperature increase at the most interesting points. These points are the real case (550ms) and the worst case of continuous transmission (396 seconds).

The graphs of time evolution of the six head tissues can be observed in Figures 5.1, 5.2, 5.3, 5.4, 5.5 and 5.6. The first point is plotted in blue (550ms) and the second point has been plotted in red (396 seconds).

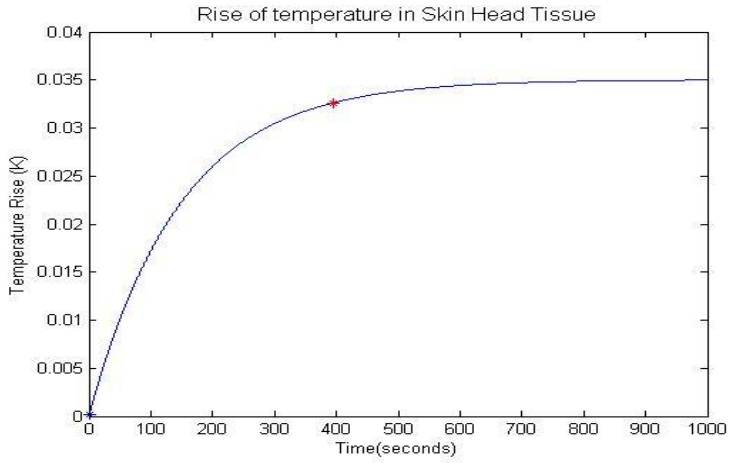

Figure V.1 Time evolution of the increase of temperature in skin head tissue

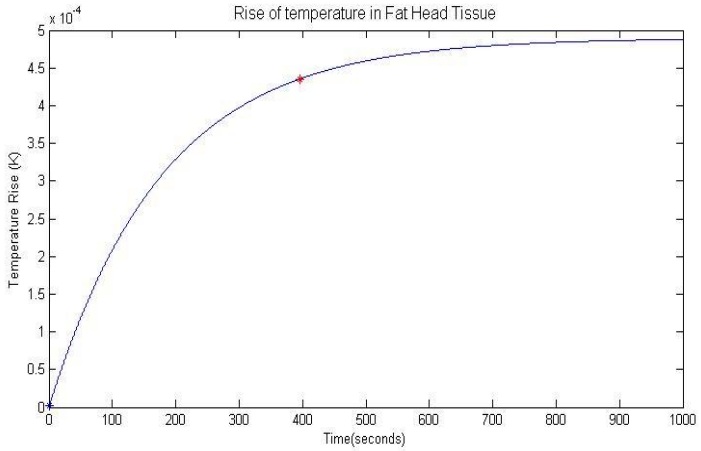

Figure V.2 Time evolution of the increase of temperature in fat head tissue

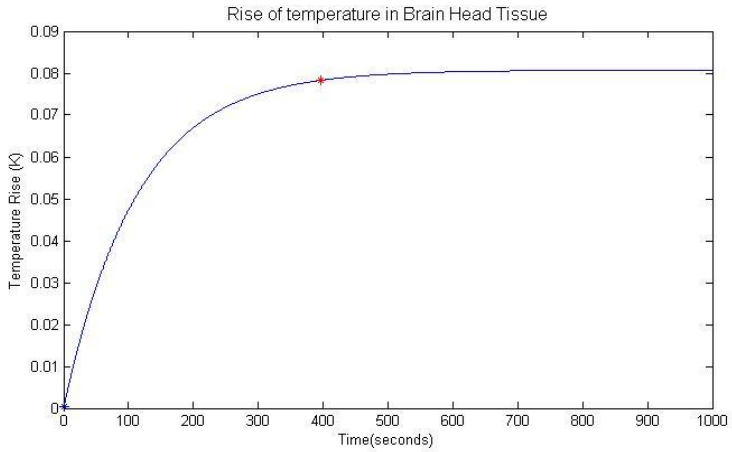

Figure V.3 Time evolution of the increase of temperature in bone head tissue

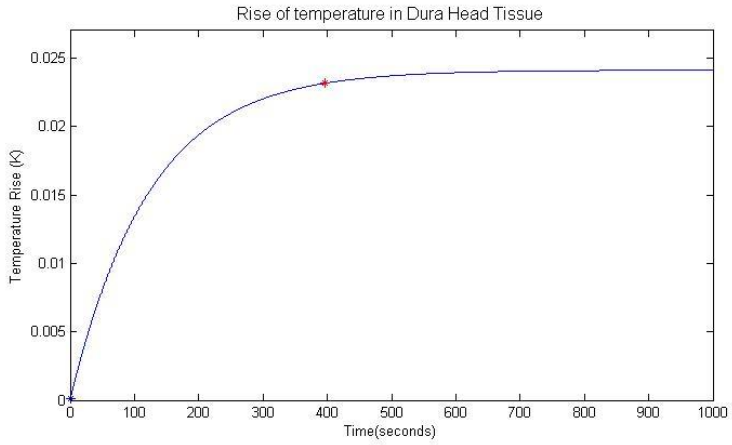

Figure V.4 Time evolution of the increase of temperature in dura head tissue

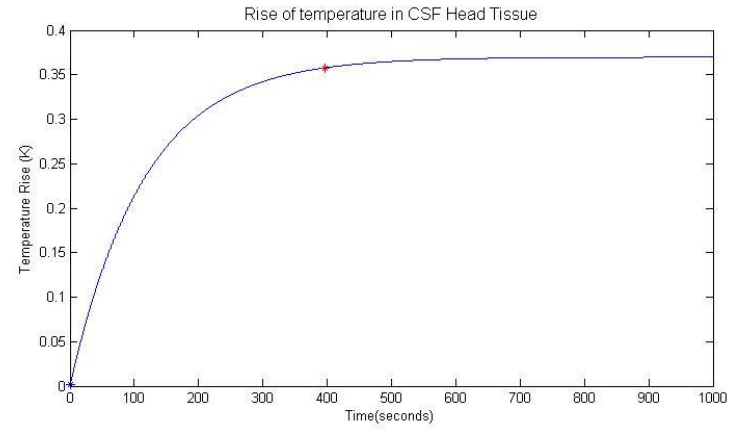

Figure V.5 Time evolution of the increase of temperature in CSF head tissue

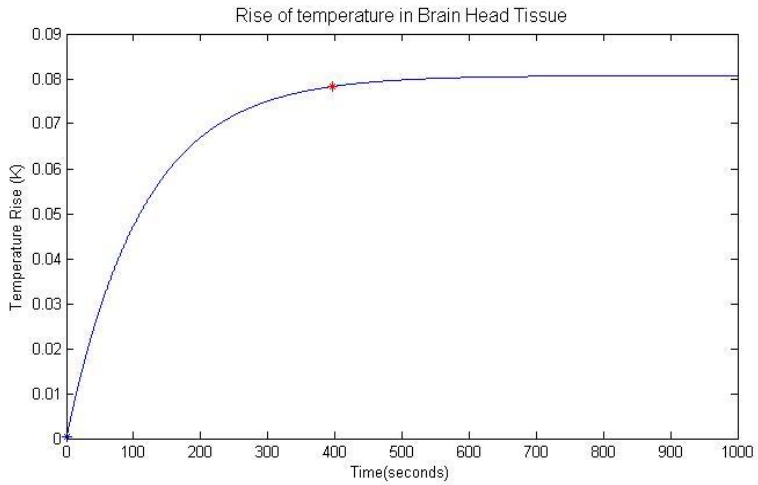

Figure V.6 Time evolution of the increase of temperature in brain head tissue

In the figures above, it can be seen how, in the cases of Brain tissue and Bone tissue, the rise of temperature at 396 seconds is almost the maximum value. Dura and Cerebrospinal Fluid are also close to the maxim value at 396 seconds. In case of Skin and Fat, the temperature value at 396 seconds appears farther from the maximum value, in the transient curve. It is also really interesting to see that all the graphs have a steady state, when the maximum rise of temperature is approached. After that, all the tissues rises of temperature are constant in function of time.

In order to see the three most significant points of $T_1(t)$, Table WWW presents the rise of temperatures in these three points: at 550ms, at 6.6 minutes and the maximum value.

Tissue	Temperature Rise at 0.55 seconds (K)	Temperature Rise at 6.6 minutes (K)	Maximum Temperature Rise (K)
Brain	3.91E-04	0.078	8.1E-02
CSF	**1.80E-03**	**0.3577**	**3.70E-01**
Dura	1.07E-04	0.0231	2.40E-02
Bone	1.94E-06	2.34E-04	3.30E-04
Fat	1.49E-06	4.35E-04	4.90E-04
Skin	1.30E-04	0.0326	3.50E-02

Table V.9 Temperature Rise of the six tissues in 3 different time values.

In the table above it can be seen that the most affected head tissue is Cerebrospinal fluid with a value of 0.3577K in case that the antenna was radiating at 406MHz and 5 W during 396 seconds. The second tissue most affected by radiation is Brain, with a temperature rise of 0.078K. On the other hand, Fat and Bone are the head tissues with less temperature increase.

Comparison between linear equation and bio-heat equation

Finally, a comparison between the linear case approximation (Section 5.1.2) and the values obtained using the Bio Heat equation time evolution is presented. As shown before, it has been possible to obtain the rise temperature when t=550ms. This was the greatest value obtained using the linear relation between SAR and increase of temperature. The goal of this comparison is to conclude if the linear approximation is a trustable method in case of short time exposure.

Table 5.10 shows the comparison between both methods at 550ms. The third column presents the difference between both values, the absolute error. The fourth column shows the relative error between both methods.

Tissue	Linear Equation (K)	Bio Heat Equation (K)	Difference (Absolute Error)	Relative Error (%)
Brain	0.00039	3.91E-04	1.00E-06	2.56E-01
CSF	**0.00175**	0.0018	5.00E-05	2.86E+00
Dura	1.08E-04	1.07E-04	5.70E-07	5.28E-01
Bone	2.72E-06	1.94E-06	7.81E-07	**2.87E+01**
Fat	1.49E-06	1.49E-06	2.50E-09	1.68E-01
Skin	1.30E-04	1.30E-04	1.60E-07	1.23E-01

Table V.10 Comparison of rise temperatures at 550ms using linear relation and using the bio-heat equation

As it can be seen in the table, all the relative errors except for CSF and Bone are below the 1%. In case of Bone, the error obtained is 28.7% which is a high error value. It means that for all the tissues, except for the Bone Head tissue, the linear relation between increase of temperature and SAR value ($\Delta T = SAR \cdot \frac{\Delta t}{c}$) is really similar to the Bio Heat transient equation ($T_1(t)$). For all the tissues except Bone, the relative error between both methods is less than 3%.

It can be concluded, that for short time exposure and for almost every head tissues, the linear equation is really close to the values obtained using the Bio Heat Equation presented in [27].

VI. Results III. Other results

In this chapter there are some other interesting results related with SAR and source power. The results presented show the relation between these two measures and are about the arm tissues.

6.1 Arm tissues. Power vs. SAR

In order to know how the SAR levels of arm tissues change are depending on the source power, the simulations at 406MHz and 1575MHz have been repeated changing the power source each time. For the distress signal frequency, the range of source power simulated has been from 1 to 10W. For the GPS frequency, the range of source power simulated has been from 0.1mW to 50mW.

The SAR levels obtained at 406MHz are shown in Table 6.1 (Average SAR) and Table 6.2 (Local SAR). In addition, the results have been plotted obtaining SAR level (Y axis) for each source power value (X axis). The plots are presented in Figures 6.1, 6.2, 6.3 and 6.4.

Power (W)	1	2	3	4	5	6	**10**
Bone	0.003	0.007	0.01	0.014	0.017	0.021	0.034
Blood	0.135	0.272	0.407	0.543	0.678	0.811	1.352
Nerve	2.035	4.07	6.105	8.14	10.175	12.221	20.353
Muscle	3.683	7.327	10.991	14.655	18.318	22.1	36.683
Fat	0.119	0.239	0.358	0.477	0.5967	0.714	1.19
Skin	16.935	33.869	50.804	67.739	84.674	101.3	168.84

Table VI.1 Average SAR for 1 to 10 W at 406MHz

Power (W)	1	2	3	4	5	6	**10**
Bone	0.005	0.009	0.014	0.019	0.024	0.029	0.049
Blood	1.922	3.8433	5.764	7.687	6.531	7.8367	13.061
Nerve	24.021	48.042	72.062	96.083	81.674	98.009	163.35
Muscle	3.979	7.9586	11.193	15.917	19.571	23.485	39.142
Fat	0.253	0.507	0.76	1.013	1.264	1.517	2.253
Skin	61.695	123.39	185.08	246.78	319.22	383.07	638.45

Table VI.2 Local SAR for 0.1 to 50mW at 406MHz

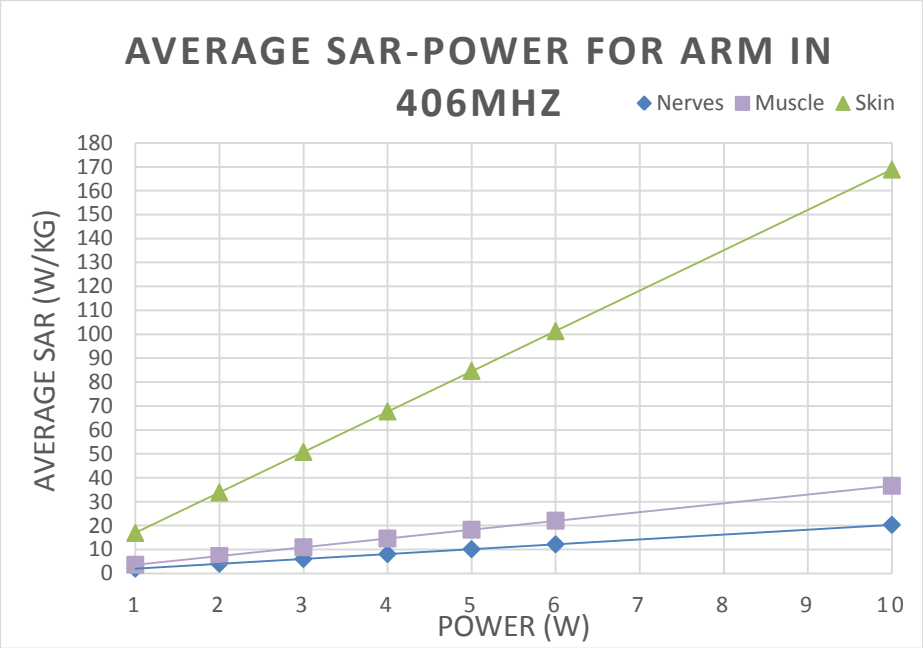

Figure VI.1 Average SAR vs Power of the three most affected arm tissues at 406MHz

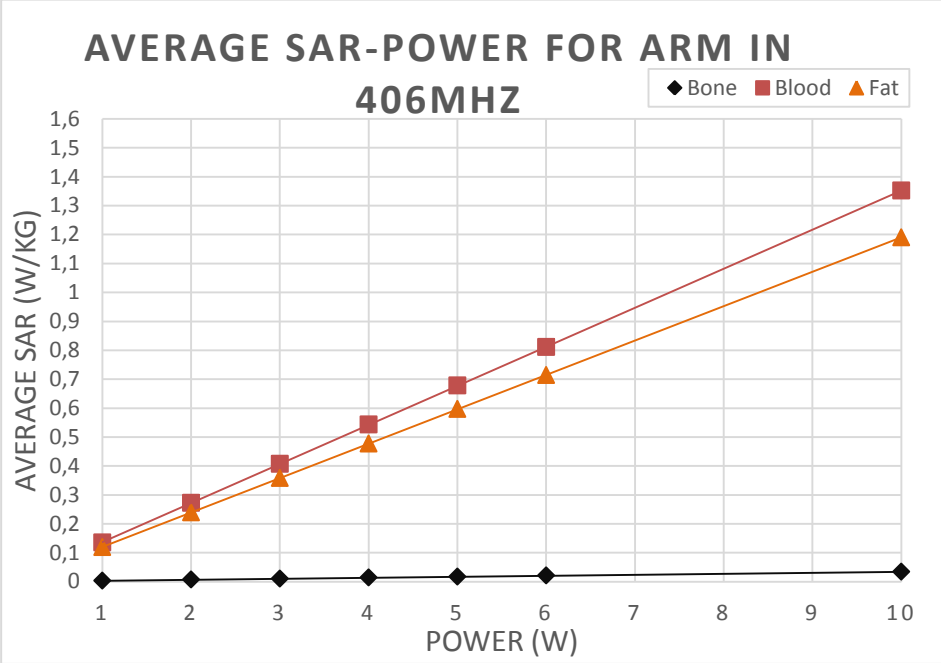

Figure VI.2 Average SAR vs Power of the three other arm tissues at 406MHz

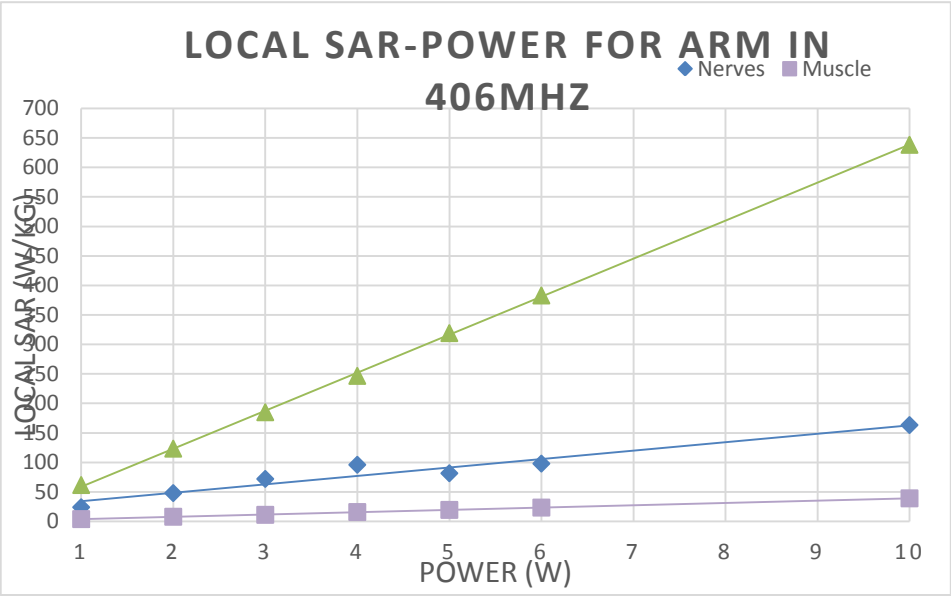

Figure VI.3 Local SAR vs Power of the three most affected arm tissues at 406MHz

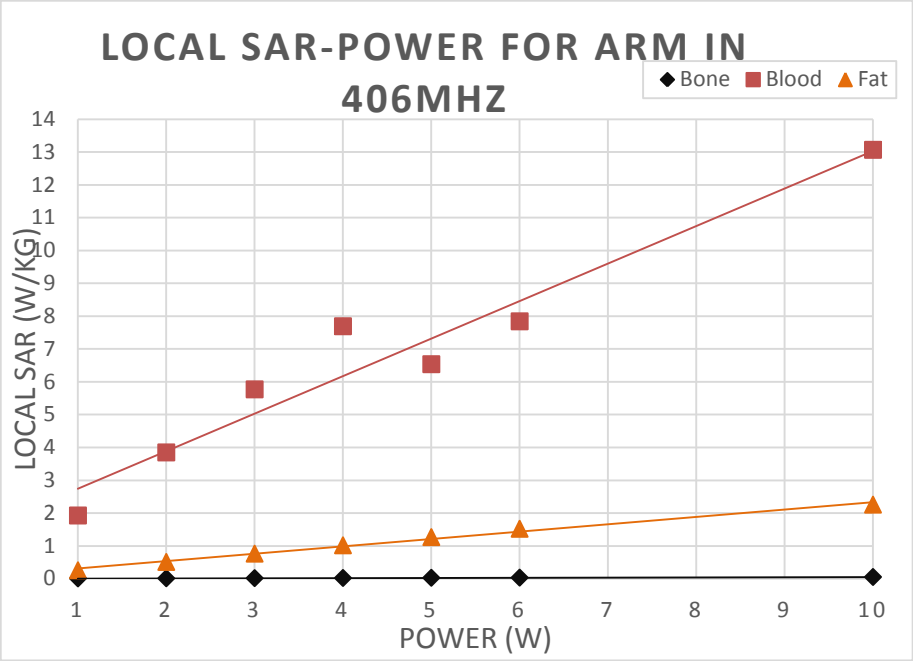

Figure VI.4 Local SAR vs Power of the three other arm tissues at 406MHz

Observing Table 6.1 and Figures 6.1 and 6.2, it can be concluded that there is a linear relationship between the source power and the average SAR levels at 406MHz. Skin is again the tissue most affected for all the range of source power followed by muscle and nerves. The points in the graphs show the SAR level and the lines crossing the

points are trend line added afterwards. The trend line is useful to see, that the evolution of SAR in function of source power is linear.

In the case of local SAR (table 6.2 and Figures 6.3 and 6.4) the results are quite different. Nerve have 3 SAR levels that are not following the trend line, even they are close. The worst case is blood (red points and line, Figure 20). In this case the relation between local SAR and source power is not linear.

The same procedure has been followed at the GPS frequency. The results obtained of SAR over source power are presented in Table 5.4 and 5.5. In addition Figures 5.6, 5.7, 5.8 and 5.9 show the evolution of the SAR levels at 1575MHz.

Power (W)	0.0001	0.0005	0.001	0.005	0.01	0.05
Bone	1.76E-04	8.78E-04	1.76E-03	8.78E-03	1.76E-02	8.78E-02
Blood	5.49E-04	2.75E-03	5.49E-03	2.75E-02	5.49E-02	2.75E-01
Nerve	5.71E-05	2.85E-04	5.71E-04	2.85E-03	5.71E-03	2.85E-02
Muscle	2.61E-04	1.31E-03	2.61E-03	1.31E-02	2.61E-02	1.30E-01
Fat	7.29E-04	3.64E-03	**7.29E-03**	3.64E-02	7.29E-02	3.64E-01
Skin	1.27E-04	9.72E-04	1.27E-03	6.33E-03	1.27E-02	6.33E-02

Table VI.3 Average SAR for 0.1 to 50mW at 1575MHz

Power (W)	0.0001	0.0005	0.001	0.005	0.01	0.05
Bone	3.25E-04	1.62E-03	3.25E-03	1.62E-02	3.25E-02	1.62E-01
Blood	9.72E-04	4.86E-03	9.73E-03	4.86E-02	9.72E-02	4.86E-01
Nerve	2.35E-04	1.17E-03	2.35E-03	1.17E-02	2.35E-02	1.17E-01
Muscle	5.31E-04	2.65E-03	5.91E-03	2.65E-02	5.07E-02	2.65E-01
Fat	3.30E-03	1.65E-02	3.30E-02	1.65E-01	3.30E-01	1.648
Skin	5.49E-04	3.05E-03	6.01E-03	3.04E-02	6.09E-02	3.04E-01

Table VI.4 Local SAR for 0.1 to 50mW at 1575MHz

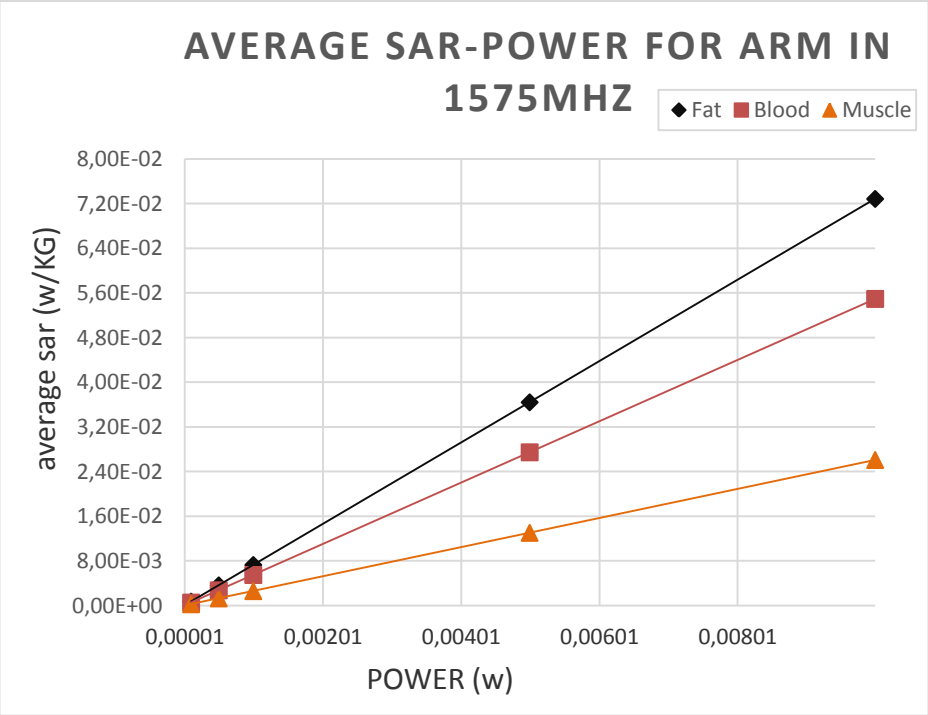

Figure VI.5 Average SAR vs Power of the three most affected arm tissues at 1575MHz

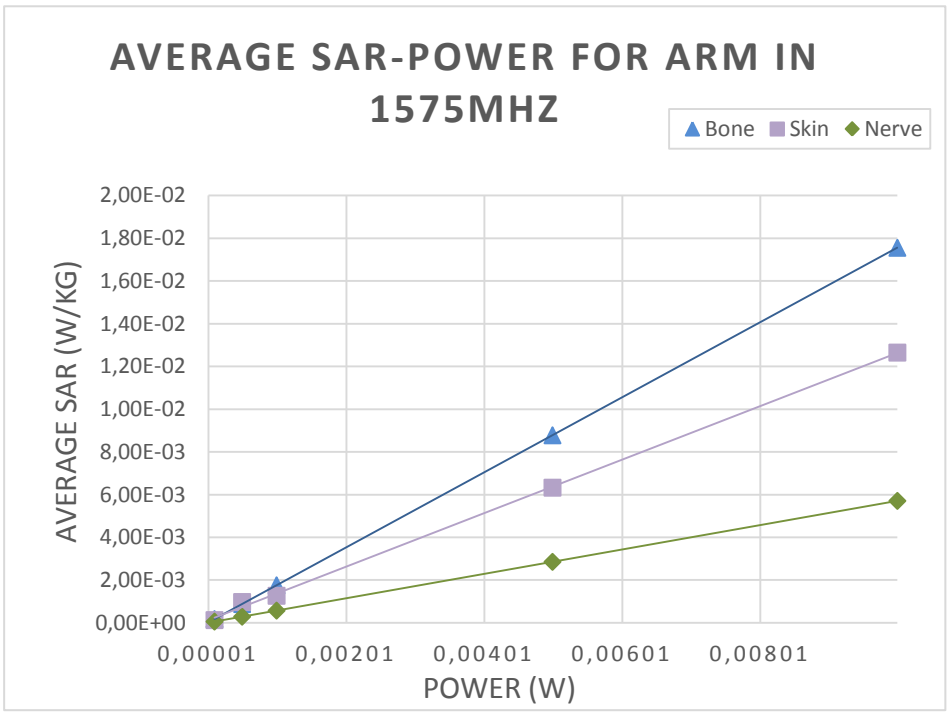

Figure VI.6 Average SAR vs Power of the three other arm tissues at 1575MHz

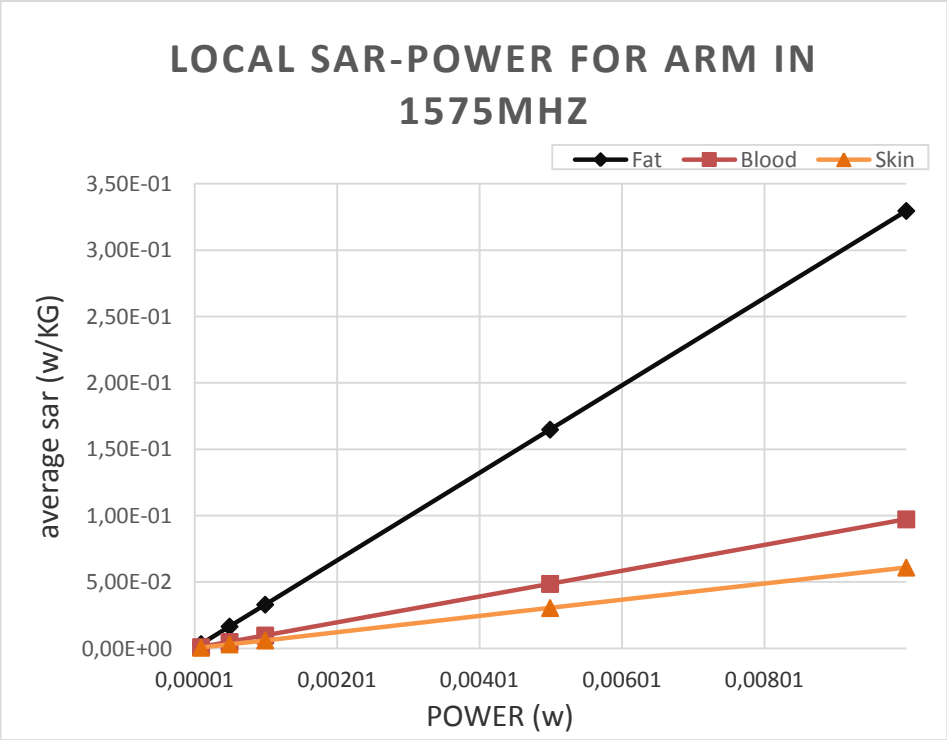

Figure VI.7 . Local SAR vs Power of the three most affected arm tissues at 1575MHz

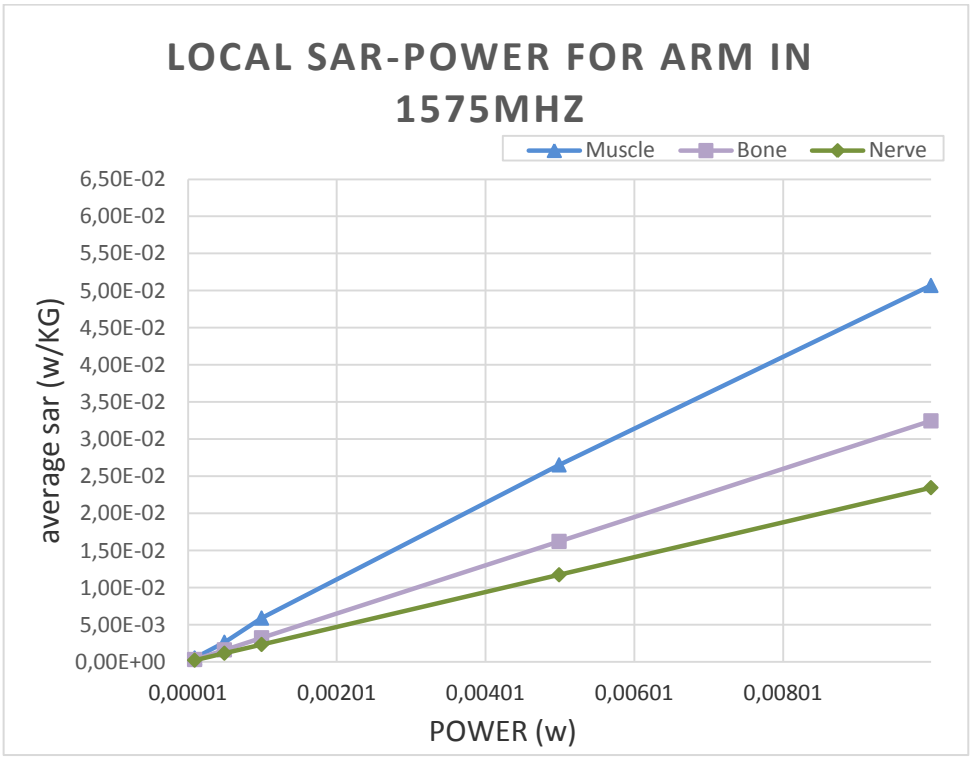

Figure VI.8 Local SAR vs Power of the three other arm tissues at 1575MHz

The results at the GPS frequency are quite different than at 406MHz. First of all, at this frequency, all the tissues have a linear relation between SAR and source power, even local SAR results. Furthermore, the three most affected tissues at 1575MHz are fat, blood and muscle regarding the average SAR results. In case of local SAR, the most affected tissues are fat, blood and skin.

Finally, observing Table 6.3, even in case of having a receiving power of 50mW (the real case is 1mW), the average SAR levels would be below the SAR U.S. limit at 1575MHz.

In conclusion, almost all the results show that the relation between SAR and power is linear. This is due to the fact that power is proportional to the square of the electrical field. SAR is equal to the square of the electrical field multiplied by conductivity and divided by mass density. Thus, the relation between SAR and power is linear, as it could be expected.

VII. CONCLUSIONS AND FUTURE WORK

In this project a deep study of Mr. Alkhamis' wearable dual-bad antenna has been done. It has been possible to reproduce the antenna in HFSS, to simulate it together with different parts of the human body and to analyze the results obtained.

Regarding the SAR results (Chapter IV), it has been possible to obtain local and average SAR for two different parts of the body, arm and head. All the average SAR levels have been calculated following the U.S. standard, which is averaging SAR over 1 gram of the tissue.

The SAR levels obtained in arm tissues are, in general, higher than the SAR levels obtained in head tissues. This is due to the fact that arm tissues are surrounded and touching by the pi-shaped antenna. For arm tissues, the most affected tissue is skin, with an average SAR clearly above the U.S. limit at the distress transmission frequency, 406MHz. Muscle and nerves also have average SAR levels above the U.S. SAR limit.

In head, the most affected tissues are cerebrospinal fluid and brain. At 406MHz, the average SAR values of both tissues are above the U.S. SAR limit. Finally, in case of having both body parts together, the SAR levels change. In general, all the average SAR values decrease in case of simulating both body parts together.

The first conclusion is that the antenna can cause high SAR levels above the U.S. limits in the arm and head tissues at 406MHz. Even though, high SAR levels do not mean necessarily that these tissues could be damaged by the pi-shaped antenna EM fields.

To be able to conclude if the antenna radiation is totally safe for human use, it was necessary to study the increase of temperature of the affected tissues. It has been possible to obtain the increase of temperature produced during the real transmission time of the antenna (550ms and 406MHz).

The increase of temperature produced in arm and head tissues due to the EM fields of the antenna are not even close to the limit of temperature increase considered dangerous. The maximum increase of temperature is produced in skin of arm and in CSF (considering the temperature increase from the average SAR).

In addition, for head tissues, it has been possible to obtain the temperature increase of tissues in long times of exposures. The increase of temperature of head tissues have been obtained considering the worst transmission case of the pi-shaped antenna (6.6 minutes at 406MHz).

The main conclusion is that, for the real time of exposure, and even for the worst possible exposure time, the temperature rise caused in the human tissues are not close to the dangerous limits. Thus, the wrist wearable dual-band antenna designed and manufactured by Rifaah Zaki Alkhamis is totally safe for arm and head tissues.

About this subject there is still a lot of work to do. It would be could interesting to study deeper the increase of temperature in longer time exposure in the arm tissues. Also, it would be important to analyze deeper the differences between SAR levels when head and arm are simulated together.

In addition, there are other body parts, also close to the antenna, that could be studied in the future. HFSS has a human body that could be really interesting to use in order to study other body parts and to study head and arm tissues deeper.

Finally, it would be really important to do real measurements of the pi-shaped antenna too. It exists the possibility to build a phantom model and then obtain the SAR levels and the temperature increase of the different tissues modeled.

References

[1] [Wikipedia, Radiation, http://en.wikipedia.org/wiki/Radiation]

[2] [Definicion.de, Radiacion, http://definicion.de/radiacion/]

[3] [U.S. Environmental Protection Energy, Radiation Protection, http://www.epa.gov/rpdweb00/understand/ionize_nonionize.html#ionizing]

[4] [Mobile phone radiation and health, http://en.wikipedia.org/wiki/Mobile_phone_radiation_and_health]

[5] [Frank S. Barnes, Ben Greenebaum "Bioengineering and Biophyisical Aspects of Electromagnetic Fields", retrieved 2006]

[6] [Specific Absorption Rate, Wikipedia, http://en.wikipedia.org/wiki/Specific_absorption_rate]

[7] [GSM Arena, SAR, http://www.gsmarena.com/glossary.php3?term=sar]

[8] [HFSS Definition, http://en.wikipedia.org/wiki/HFSS]

[9] [HFSS Online Help, "SAR", Ansoft HFSS 14.0.1]

[10] [Victor M. Cruz, "Riesgo para la salud por radiaciones no ionizantes de las redes de telecomunicacione sen Peru", Rev Peru Med Exp Salud Publica, retrieved 2009]

[11] [Teerapot Wassapan, Phadungsak Rattanadencho, "Specific absorption rate and temperature increase in the human eye due to electromagnetic fields exposure at different frequencies", International Journal of Heat and Mass Transfer, retrieved 2013]

[12] [PRWainwright,"The relationship of temperature rise to specific absorption rate and current in the human leg for exposure to electromagnetic radiation in the high frequency band", INSTITUTE OF PHYSICS PUBLISHING, retrieved 16 September 2003]

[13] [Paolo Bernardi*, Life Fellow, IEEE*, Marta Cavagnaro*, Member, IEEE*, Stefano Pisa*, Member, IEEE*, and,Emanuele Piuzz, "Specific Absorption Rate and Temperature Elevation in a Subject Exposed in the Far-Field of Radio-Frequency Sources Operating in the 10–900-MHz Range", IEEE TRANSACTIONS ON BIOMEDICAL ENGINEERING, retrieved March 2003]

[14] [Rifaah Zaki Alkhamis, "Global positioning system (GPS) and distress signal frequency wrist wearable dual-band antenna", UCCS, retrieved July 2013]

[15][FCFM, Valeria Tapia L. y Patricio Mena M, Manual introductorio a HFSS, retrieved 2010]

[16] [HFSS TUTORIAL, Design of a Loop Inductor]

[17][ANSYS, Inc.,"Getting Started with HFSS: A Probe Patch Feed Antenna", retrieved May 2010]

[18][Ansoft Corporation, "Getting Started with HFSS v9 for Antenna Design", retrieved October 2003]

[19] [Ansoft Corporation, "Ansoft HFSS User's Guide. High Frequency Structure Simulator"]

[20] [Singularity Hub, "Team of doctors succesfully perform double arm transplant on veteran", http://singularityhub.com/, retrieved February 2013]

[21] [IFAC, "Dielectric properties of body tissues", http://niremf.ifac.cnr.it/tissprop/]

[22] [Om P. Gandi, Gianluca Lazzi, Cynthia M. Furse, "Electromagnetic Absorption in the Human Head and neck for Mobile Telephones at 835 and 1900 MHz", IEEE TRANSACTIONS ON MICROWAVE THEROY AND TECNIQUES, retrieved October 1996]

[23] [Adel Z. El Dein, Alaeddin Amr,"Specific Absorption Rate (SAR) Induced in Human Heads of Various Sizes When Using a Mobile Phone", retrieved June 2010]

[24] [Dr. Prsasad, "Acoustic Neuroma", http://www.earsite.com/acoustic-neuroma-treatment]

[25] [Asma Lak, Homayoon Oraizi,"Evaluation of SAR Distribution in Six-Layer Human Head Model", Hindawi Publishing Corporation, retrieved Agust 2012]

[26] [IT IS Foundation, http://www.itis.ethz.ch/itis-for-health/tissue-properties/database/heat-capacity/]

[27] [H.N. KRITIKOS, HERMAN P. SCHWAN, "Potential Temperature Rise Induced by Electromagetic Field in Brain Tissues", retrieved January 1979]